

# Electroweak breaking and neutrino mass: “invisible” Higgs decays at the LHC (Type II seesaw)

Cesar Bonilla,<sup>1,\*</sup> Jorge C. Romão,<sup>2,†</sup> and José W. F. Valle<sup>1,‡</sup>

<sup>1</sup> *AHEP Group, Instituto de Física Corpuscular – C.S.I.C./Universitat de València  
Edificio de Institutos de Paterna, C/Catedrático José  
Beltrán, 2 E-46980 Paterna (València) - SPAIN*

<sup>2</sup> *Departamento de Física and CFTP, Instituto Superior Técnico  
Universidade de Lisboa, Av. Rovisco Pais 1, 1049-001 Lisboa, Portugal*

## Abstract

Neutrino mass generation through the Higgs mechanism not only suggests the need to reconsider the physics of electroweak symmetry breaking from a new perspective, but also provides a new theoretically consistent and experimentally viable paradigm. We illustrate this by describing the main features of the electroweak symmetry breaking sector of the simplest type-II seesaw model with spontaneous breaking of lepton number. After reviewing the relevant “theoretical” and astrophysical restrictions on the Higgs sector, we perform an analysis of the sensitivities of Higgs boson searches at the ongoing ATLAS and CMS experiments at the LHC, including not only the new contributions to the decay channels present in the Standard Model (SM) but also genuinely non-SM Higgs boson decays, such as “invisible” Higgs boson decays to majorons. We find sensitivities that are likely to be reached at the upcoming Run of the experiments.

PACS numbers: 14.60.Pq 12.60.Fr 14.60.St

---

\*Electronic address: cesar.bonilla@ific.uv.es

†Electronic address: jorge.romao@tecnico.ulisboa.pt

‡Electronic address: valle@ific.uv.es

## I. INTRODUCTION

The electroweak breaking sector is a fundamental ingredient of the Standard Model many of whose detailed properties remain open, even after the historic discovery of the Higgs boson [1, 2]. The electroweak breaking sector is subject to many restrictions following from direct experimental searches at colliders [3, 4], as well as global fits [5, 6] of precision observables [7–9]. Moreover, its properties are may also be restricted by theoretical consistency arguments, such as naturalness, perturbativity and stability [10]. The latter have long provided strong motivation for extensions of the Standard Model such as those based on the idea of supersymmetry.

Following the approach recently suggested in Refs. [11, 12] we propose to take seriously the hints from the neutrino mass generation scenario to the structure of the scalar sector. In particular, the most accepted scenario of neutrino mass generation associates the smallness of neutrino mass to their charge neutrality which suggests them to be of Majorana nature due to some, currently unknown, mechanism of lepton number violation. The latter requires an extension of the  $SU(3)_c \otimes SU(2)_L \otimes U(1)_Y$  Higgs sector and hence the need to reconsider the physics of symmetry breaking from a new perspective. In broad terms this would provide an alternative to supersymmetry as paradigm of electroweak breaking. Amongst its other characteristic features is the presence of doubly charged scalar bosons, compressed mass spectra of heavy scalars dictated by stability and perturbativity and the presence of “invisible” decays of Higgs bosons to the Nambu-Goldstone boson associated to spontaneous lepton number violation and neutrino mass generation [13].

In this paper we study the invisible decays of the Higgs bosons in the context of a type-II seesaw majoron model [14] in which the neutrino mass is generated after spontaneous violation of lepton number at some low energy scale,  $\Lambda_{EW} \lesssim \Lambda \sim \mathcal{O}(\text{TeV})$  [15, 16]<sup>1</sup>. This scheme requires the presence of two lepton number-carrying scalar multiplets in the extended  $SU(3)_c \otimes SU(2)_L \otimes U(1)_Y$  model, a singlet  $\sigma$  and a triplet  $\Delta$  under  $SU(2)$  – this seesaw scheme was called “123”-seesaw model in [14] and here we take the “pure” version of this scheme, without right-handed neutrinos. The presence of the new scalars implies the existence of new contributions to “visible” SM Higgs decays, such as the  $h \rightarrow \gamma\gamma$  decay channel, in addition to intrinsically new Higgs decay channels involving the emission of majorons, such as the “invisible” decays of the CP-even scalar bosons. As a result, one can set upper limits on the invisible decay channel based on the available data which restrict the “visible” channels.

The plan of this paper is as follows. In the next section we describe the main features of

---

<sup>1</sup> The idea of the Majoron was first proposed in [17] though in the framework of the Type I seesaw, not relevant for our current paper. On the other hand the triplet Majoron was suggested in [18] but has been ruled out since the first measurements of the invisible Z width by the LEP experiments. Regarding the idea of invisible Higgs decays was first given in Ref. [19], though the early scenarios have been ruled out.

the symmetry breaking sector of the “123” type II seesaw model. In section III we discuss the “theoretical” and astrophysical constraints relevant for the Higgs sector. Taking these into account, we study the sensitivities of Higgs boson searches at the LHC to Standard Model scalar boson decays in section IV. Section V addresses the non-SM Higgs decays of the model. Section VI summarizes our results and we conclude in section VII.

## II. THE TYPE-II SEESAW MODEL

Our basic framework is the “123” seesaw scheme originally proposed in Ref. [14] whose Higgs sector contains, in addition to the  $SU(3)_c \otimes SU(2)_L \otimes U(1)_Y$  scalar doublet  $\Phi$ , two lepton-number-carrying scalars: a complex singlet  $\sigma$  and a triplet  $\Delta$ . All these fields develop non-zero vacuum expectation values (vevs) leading to the breaking of the Standard Model (SM) gauge group as well as the global symmetry  $U(1)_L$  associated to lepton number. The latter breaking accounts for generation of the small neutrino masses. Therefore, the scalar sector is given by

$$\Phi = \begin{bmatrix} \phi^0 \\ \phi^- \end{bmatrix} \quad \text{and} \quad \Delta = \begin{bmatrix} \Delta^0 & \frac{\Delta^+}{\sqrt{2}} \\ \frac{\Delta^+}{\sqrt{2}} & \Delta^{++} \end{bmatrix} \quad (1)$$

with  $L = 0$  and  $L = -2$ , respectively, and the scalar field  $\sigma$  with lepton number  $L = 2$ . Below we will consider the required vev hierarchies in the model.

### A. Yukawa Sector

Here we consider the simplest version of the seesaw scheme proposed in Ref. [14] in which no right-handed neutrinos are added, and only the  $SU(3)_c \otimes SU(2)_L \otimes U(1)_Y$  electroweak breaking sector is extended so as to spontaneously break lepton number giving mass to neutrinos. Such “123” majoron–seesaw model is described by the  $SU(3)_c \otimes SU(2)_L \otimes U(1)_Y \otimes U(1)_L$  invariant Yukawa Lagrangian,

$$\mathcal{L}_Y = y_{ij}^d \bar{Q}_i u_{Rj} \Phi + y_{ij}^u \bar{Q}_i d_{Rj} \tilde{\Phi} + y_{ij}^\ell \bar{L}_i \ell_{Rj} \Phi + y_{ij}^\nu L_i^T C \Delta L_j + \text{h.c.} \quad (2)$$

In this model the neutrino mass (see Fig. 1) is given by,

$$m_\nu = y^\nu \kappa v_1 \frac{v_2^2}{m_\Delta^2} \quad (3)$$

where  $v_1$  and  $v_2$  are the vevs of the singlet and the doublet, respectively. Here  $\kappa$  is a dimensionless parameter that describes the interaction amongst the three scalar fields (see below), and  $m_\Delta$  is the mass of the scalar triplet  $\Delta$ .

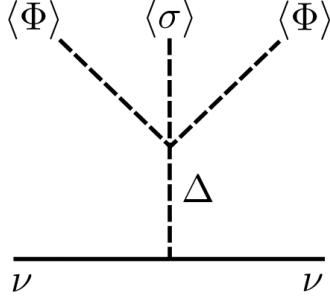


Figure 1: Diagram that generates non-zero neutrino mass in the model.

At this point we note that the smallness of neutrino mass i.e.

$$m_\nu \lesssim 1 \text{ eV}$$

may define interesting regions of the parameter space in any neutrino mass generation model where the new physics is expected to be hidden from direct observation. In particular, we are interested in spotting those regions accessible at collider searches such as the ongoing experiments at the LHC (see Ref. [20] and references therein).

In our pure type II seesaw model where lepton number is spontaneously violated at some low energy scale we have

$$m_\nu = y^\nu \langle \Delta \rangle$$

with the effective vev is given as  $\langle \Delta \rangle = \mu \langle \Phi \rangle^2 / M_\Delta^2$  where  $\Delta$  is the isotriplet lepton-number-carrying scalar. Here  $\langle \Phi \rangle$  is fixed by the mass of the  $W$  boson and

$$\mu = \kappa v_1$$

is the dimensionful parameter responsible of lepton number violation, see eq. (3). Therefore if  $y^\nu \sim \mathcal{O}(1)$  and the mass  $M_\Delta$  lies at 1 TeV region then one has that  $\langle \Delta \rangle \sim m_\nu$  and  $\mu \sim 1 \text{ eV}$ . Note that one may consider two situations:  $v_1 \gg \Lambda_{EW}$  (high-scale seesaw mechanism) in whose case the scalar singlet and the invisible decays of the Higgs are decoupled [15]; the second interesting case is when  $\Lambda_{EW} \lesssim v_1 \lesssim \text{few TeV}$  (low-scale seesaw mechanism). In this case the parameter  $\kappa$  is the range  $[10^{-14}, 10^{-16}]$  for  $y^\nu \sim \mathcal{O}(1)$ . In this case one has new physics at the TeV region including the “invisible” decays of the Higgs bosons.

Therefore, led by the smallness of the neutrino mass we can qualitatively determine that the analysis to be carried out is characterized by having a vev hierarchy

$$v_1 \gtrsim v_2 \gg v_3$$

and the smallness of the coupling  $\kappa$ , that is  $\kappa \ll 1$ .

## B. The scalar potential

The scalar potential invariant under the  $SU(3)_c \otimes SU(2)_L \otimes U(1)_Y \otimes U(1)_L$  symmetry is given by [15, 16]<sup>2</sup>

$$\begin{aligned} V = & \mu_1^2 \sigma^* \sigma + \mu_2^2 \Phi^\dagger \Phi + \mu_3^2 \text{tr}(\Delta^\dagger \Delta) + \lambda_1 (\Phi^\dagger \Phi)^2 + \lambda_2 [\text{tr}(\Delta^\dagger \Delta)]^2 \\ & + \lambda_3 \Phi^\dagger \Phi \text{tr}(\Delta^\dagger \Delta) + \lambda_4 \text{tr}(\Delta^\dagger \Delta \Delta^\dagger \Delta) + \lambda_5 (\Phi^\dagger \Delta^\dagger \Delta \Phi) + \beta_1 (\sigma^* \sigma)^2 \\ & + \beta_2 (\Phi^\dagger \Phi)(\sigma^* \sigma) + \beta_3 \text{tr}(\Delta^\dagger \Delta)(\sigma^* \sigma) - \kappa (\Phi^T \Delta \Phi \sigma + \text{h.c.}). \end{aligned} \quad (4)$$

As mentioned above the scalar fields  $\sigma$ ,  $\phi$  and  $\Delta$  acquire non-zero vacuum expectation values,  $v_1$ ,  $v_2$  and  $v_3$ , respectively, so that, they can be shifted as follows,

$$\begin{aligned} \sigma &= \frac{v_1}{\sqrt{2}} + \frac{R_1 + iI_1}{\sqrt{2}}, \\ \phi^0 &= \frac{v_2}{\sqrt{2}} + \frac{R_2 + iI_2}{\sqrt{2}}, \\ \Delta^0 &= \frac{v_3}{\sqrt{2}} + \frac{R_3 + iI_3}{\sqrt{2}}. \end{aligned}$$

The minimization conditions of eq. (4) are given by,

$$\begin{aligned} \mu_1^2 &= \frac{-2\beta_1 v_1^3 - \beta_2 v_1 v_2^2 - \beta_3 v_1 v_3^2 + \kappa v_2^2 v_3}{2v_1}, \\ \mu_2^2 &= -\frac{1}{2} \left( 2\lambda_1 v_2^2 + \beta_2 v_1^2 + (\lambda_3 + \lambda_5) v_3^2 - 2\kappa v_1 v_3 \right), \\ \mu_3^2 &= \frac{-2(\lambda_2 + \lambda_4) v_3^3 - (\lambda_3 + \lambda_5) v_2^2 v_3 - \beta_3 v_1^2 v_3 + \kappa v_1 v_2^2}{2v_3}. \end{aligned} \quad (5)$$

and from these one can derive a vev seesaw relation of the type

$$v_1 v_3 \sim \kappa v_2^2,$$

where  $\kappa$  is the dimensionless coupling that generates the mass parameter associated to the cubic term in the scalar potential of the simplest triplet seesaw scheme with explicit lepton number violation as proposed in [21] and recently revisited in [12].

## Neutral Higgs bosons

One can now write the resulting squared mass matrix for the CP-even scalars in the weak basis  $(R_1, R_2, R_3)$  as follows,

$$M_R^2 = \begin{bmatrix} 2\beta_1 v_1^2 + \frac{1}{2}\kappa v_2^2 \frac{v_3}{v_1} & \beta_2 v_1 v_2 - \kappa v_2 v_3 & \beta_3 v_1 v_3 - \frac{1}{2}\kappa v_2^2 \\ \beta_2 v_1 v_2 - \kappa v_2 v_3 & 2\lambda_1 v_2^2 & (\lambda_3 + \lambda_5) v_2 v_3 - \kappa v_1 v_2 \\ \beta_3 v_1 v_3 - \frac{1}{2}\kappa v_2^2 & (\lambda_3 + \lambda_5) v_2 v_3 - \kappa v_1 v_2 & 2(\lambda_2 + \lambda_4) v_3^2 + \frac{1}{2}\kappa v_2^2 \frac{v_1}{v_3} \end{bmatrix}. \quad (6)$$

---

<sup>2</sup> From now on we follow the notation and conventions used in Ref. [16].

The matrix  $M_R^2$  is diagonalized by an orthogonal matrix as follows,  $\mathcal{O}_R M_R^2 \mathcal{O}_R^T = \text{diag}(m_{H_1}^2, m_{H_2}^2, m_{H_3}^2)$ , where

$$\begin{pmatrix} H_1 \\ H_2 \\ H_3 \end{pmatrix} = \mathcal{O}_R \begin{pmatrix} R_1 \\ R_2 \\ R_3 \end{pmatrix}. \quad (7)$$

We use the standard parameterization  $\mathcal{O}_R = R_{23} R_{13} R_{12}$  where

$$R_{12} = \begin{pmatrix} c_{12} & s_{12} & 0 \\ -s_{12} & c_{12} & 0 \\ 0 & 0 & 1 \end{pmatrix}, \quad R_{13} = \begin{pmatrix} c_{13} & 0 & s_{13} \\ 0 & 1 & 0 \\ -s_{13} & 0 & c_{13} \end{pmatrix}, \quad R_{23} = \begin{pmatrix} 1 & 0 & 0 \\ 0 & c_{23} & s_{23} \\ 0 & -s_{23} & c_{23} \end{pmatrix} \quad (8)$$

and  $c_{ij} = \cos \alpha_{ij}$ ,  $s_{ij} = \sin \alpha_{ij}$ , so that the rotation matrix  $\mathcal{O}_R$  is re-expressed in terms of the mixing angles in the following way:

$$\mathcal{O}_R = \begin{pmatrix} c_{12}c_{13} & c_{13}s_{12} & s_{13} \\ -c_{23}s_{12} - c_{12}s_{13}s_{23} & c_{23}c_{12} - s_{12}s_{13}s_{23} & c_{13}s_{23} \\ -c_{12}c_{23}s_{13} + s_{23}s_{12} & -c_{23}s_{12}s_{13} - c_{12}s_{23} & c_{13}c_{23} \end{pmatrix}. \quad (9)$$

On the other hand, the squared mass matrix for the CP-odd scalars in the weak basis  $(I_1, I_2, I_3)$  is given as,

$$M_I^2 = \kappa \begin{bmatrix} \frac{1}{2}v_2^2 \frac{v_3}{v_1} & v_2 v_3 & \frac{1}{2}v_2^2 \\ v_2 v_3 & 2v_1 v_3 & v_1 v_2 \\ \frac{1}{2}v_2^2 & v_1 v_2 & \frac{1}{2}v_2^2 \frac{v_1}{v_3} \end{bmatrix}. \quad (10)$$

The matrix  $M_I^2$  is diagonalized as,  $\mathcal{O}_I M_I^2 \mathcal{O}_I^T = \text{diag}(0, 0, m_A^2)$ , where the null masses correspond to the would-be Goldstone boson  $G^0$  and the Majoron  $J$ , while the squared CP-odd mass is

$$m_A^2 = \kappa \left( \frac{v_2^2 v_1^2 + v_2^2 v_3^2 + 4v_3^2 v_1^2}{2v_3 v_1} \right). \quad (11)$$

The mass eigenstates are linked with the original ones by the following rotation,

$$\begin{pmatrix} A_1 \\ A_2 \\ A_3 \end{pmatrix} \equiv \begin{pmatrix} J \\ G^0 \\ A \end{pmatrix} = \mathcal{O}_I \begin{pmatrix} I_1 \\ I_2 \\ I_3 \end{pmatrix} \quad (12)$$

where the matrix  $\mathcal{O}_I$  is given by,

$$\mathcal{O}_I = \begin{bmatrix} cv_1 V^2 & -2cv_2 v_3^2 & -cv_2^2 v_3 \\ 0 & v_2/V & -2v_3/V \\ bv_2/2v_1 & b & bv_2/2v_3 \end{bmatrix}, \quad (13)$$

with

$$V^2 = v_2^2 + 4v_3^2, \quad (14)$$

$$c^{-2} = v_1^2 V^4 + 4v_2^2 v_3^4 + v_2^4 v_3^2$$

$$b^2 = \frac{4v_1^2 v_3^2}{v_2^2 v_1^2 + v_2^2 v_3^2 + 4v_3^2 v_1^2}. \quad (15)$$

### Charged Higgs bosons

The squared mass matrix for the singly-charged scalar bosons in the original weak basis  $(\phi^\pm, \Delta^\pm)$  is given by,

$$M_{H^\pm}^2 = \begin{bmatrix} \kappa v_1 v_3 - \frac{1}{2} \lambda_5 v_3^2 & \frac{1}{2\sqrt{2}} v_2 (\lambda_5 v_3 - 2\kappa v_1) \\ \frac{1}{2\sqrt{2}} v_2 (\lambda_5 v_3 - 2\kappa v_1) & \frac{1}{4v_3} v_2^2 (-\lambda_5 v_3 + 2\kappa v_1) \end{bmatrix}. \quad (16)$$

We now define

$$\begin{pmatrix} G^\pm \\ H^\pm \end{pmatrix} = \begin{pmatrix} c_\pm & s_\pm \\ -s_\pm & c_\pm \end{pmatrix} \begin{pmatrix} \phi^\pm \\ \Delta^\pm \end{pmatrix}, \quad \text{and} \quad \mathcal{O}_\pm M_{H^\pm}^2 \mathcal{O}_\pm^T = \text{diag}(0, m_{H^\pm}^2). \quad (17)$$

where  $c_\pm$  and  $s_\pm$  are given as  $c_\pm = v_2 / \sqrt{v_2^2 + 2v_3^2}$  and  $s_\pm = \sqrt{2}v_3 / \sqrt{v_2^2 + 2v_3^2}$ . The massless state corresponds to the would-be Goldstone bosons  $G^\pm$  and the massive state  $H^\pm$  is characterized by,

$$m_{H^\pm}^2 = \frac{1}{4v_3} (2\kappa v_1 - \lambda_5 v_3) (v_2^2 + 2v_3^2). \quad (18)$$

On the other hand, the doubly-charged scalars  $\Delta^{\pm\pm}$  has mass

$$m_{\Delta^{++}}^2 = \frac{1}{2v_3} (\kappa v_1 v_2^2 - 2\lambda_4 v_3^3 - \lambda_5 v_2^2 v_3). \quad (19)$$

### C. Scalar boson mass sum rules

Notice that using the fact that the smallness of the neutrino mass implies that the parameters  $\kappa$  and  $v_3$  are very small one can, to a good approximation, rewrite eq. (6) schematically in the form,

$$M_R^2 \sim \begin{pmatrix} \star & \star & 0 \\ \star & \star & 0 \\ 0 & 0 & \star \end{pmatrix} \quad \text{so that} \quad \mathcal{O}_R \sim \begin{pmatrix} c_{12} & s_{12} & 0 \\ -s_{12} & c_{12} & 0 \\ 0 & 0 & 1 \end{pmatrix}, \quad (20)$$

and eq. (11) becomes,

$$m_A^2 \sim \kappa \frac{v_2^2 v_1}{2v_3}. \quad (21)$$

As a result, the scalar  $H_3$  and the pseudo-scalar  $A$  are almost degenerate,

$$m_{H_3} = (M_R^2)_{33} \approx m_A^2. \quad (22)$$

In the same way, by using eqs. (11), (18) and (19), one can derive the following mass relations,

$$m_A^2 - m_{H^+}^2 \approx \frac{\lambda_5 v_2^2}{4} \quad \text{and} \quad 2m_{H^+}^2 - m_A^2 - m_{\Delta^{++}}^2 \approx \lambda_4 v_3^2,$$

which can be rewritten in the form,

$$m_{H^+}^2 - m_{\Delta^{++}}^2 \approx m_A^2 - m_{H^+}^2 \approx \frac{\lambda_5 v_2^2}{4}. \quad (23)$$

This sum rule is also satisfied in the Type-II seesaw model with explicit breaking of lepton number. Imposing the perturbativity condition one finds that the squared mass difference between, say doubly and singly charged scalar bosons, cannot be too large [12]. Explicit comparison shows that  $\lambda_5$  in eq. (4) corresponds to  $\lambda'_{H\Delta}$  in Ref. [12]. Therefore when the couplings of the singlet  $\sigma$  in eq. (4) are small,  $\lambda_5$  is constrained to be in the range  $[-0.85, 0.85]$ , so that the remaining couplings are kept small up to the Planck scale and vacuum stability is guaranteed. See Figure 4 in Ref. [12]. Likewise when one decouples the triplet one also recovers the results found in Ref. [11].

### III. THEORETICAL CONSTRAINTS

Before analyzing the sensitivities of the searches for Higgs bosons at the LHC experiments, we first discuss the restrictions that follow from the consistency requirements of the Higgs potential. We can rewrite the dimensionless parameters  $\lambda_{1,2,3}$  and  $\beta_{1,2,3}$  in eq. (4) in terms of the mixing angles,  $\alpha_{ij}$  and scalar the masses  $m_{H_{1,2,3}}$  by solving  $\mathcal{O}_R M_R^2 \mathcal{O}_R^T = \text{diag}(m_{H_1}^2, m_{H_2}^2, m_{H_3}^2)$  and  $\mathcal{O}_I M_I^2 \mathcal{O}_I^T = \text{diag}(0, 0, m_A^2)$ . Hence one gets,

$$\begin{aligned} \lambda_1 &= \frac{1}{2v_2^2} \left[ m_{H_1}^2 c_{13}^2 s_{12}^2 + m_{H_2}^2 (c_{12}c_{23} - s_{12}s_{13}s_{23})^2 + m_{H_3}^2 (c_{12}s_{23} + s_{12}s_{13}c_{23})^2 \right] \\ \lambda_2 &= \frac{1}{2v_3^2} \left[ m_{H_1}^2 s_{13}^2 + c_{13}^2 (m_{H_2}^2 s_{23}^2 + m_{H_3}^2 c_{23}^2) \right] - \left( \lambda_4 + \kappa \frac{v_1 v_2^2}{4v_3^3} \right) \\ \lambda_3 &= \frac{c_{13}}{v_2 v_3} \left[ m_{H_1}^2 s_{12}s_{13} + m_{H_2}^2 s_{23} (c_{12}c_{23} - s_{12}s_{13}s_{23}) - m_{H_3}^2 c_{23} (c_{12}s_{23} + s_{12}s_{13}c_{23}) \right] \\ &\quad - \left( \lambda_5 - \kappa \frac{v_1}{v_3} \right) \\ \beta_1 &= \frac{1}{2v_1^2} \left[ m_{H_1}^2 c_{12}^2 c_{13}^2 + m_{H_2}^2 (s_{12}c_{23} + c_{12}s_{23}s_{13})^2 + m_{H_3}^2 (s_{12}s_{23} - c_{12}c_{23}s_{13})^2 \right] - \kappa \frac{v_2^2 v_3}{4v_1^3} \\ \beta_2 &= \frac{1}{v_1 v_2} \left[ m_{H_1}^2 c_{12}s_{12}c_{13}^2 - m_{H_2}^2 (c_{23}s_{12} + c_{12}s_{13}s_{23})(c_{12}c_{23} - s_{12}s_{13}s_{23}) \right. \\ &\quad \left. - m_{H_3}^2 (s_{23}s_{12} - c_{12}s_{13}c_{23})(c_{12}s_{23} + s_{12}s_{13}c_{23}) \right] + \kappa \frac{v_3}{v_1} \\ \beta_3 &= \frac{c_{13}}{v_1 v_3} \left[ m_{H_1}^2 c_{12}s_{13} - m_{H_2}^2 s_{23}(s_{12}c_{23} + c_{12}s_{13}s_{23}) + m_{H_3}^2 c_{23}(s_{12}s_{23} - c_{12}s_{13}c_{23}) \right] + \kappa \frac{v_2^2}{2v_1 v_3}. \end{aligned}$$

In addition, using eqs. (11), (18) and (19) we can write the dimensionless parameters  $\lambda_{4,5}$  and  $\kappa$  as functions of the vevs  $v_{1,2,3}$  and the masses of the pseudo-, singly- and doubly-charged scalar bosons (i.e.  $m_A$ ,  $m_{H^\pm}$  and  $m_{\Delta^{\pm\pm}}$ , respectively) as,

$$\begin{aligned}\lambda_4 &= \frac{1}{v_3^2} \left( 2m_{H^\pm}^2 \frac{v_2^2}{v_2^2 + 2v_3^2} - m_A^2 \frac{v_1^2 v_2^2}{v_2^2 v_3^2 + v_1^2 (v_2^2 + 4v_3^2)} - m_{\Delta^{\pm\pm}}^2 \right) \\ \lambda_5 &= \left( -4m_{H^\pm}^2 \frac{1}{v_2^2 + 2v_3^2} + 4m_A^2 \frac{v_1^2}{v_2^2 v_3^2 + v_1^2 (v_2^2 + 4v_3^2)} \right) \\ \kappa &= 2m_A^2 \frac{v_1 v_3}{v_2^2 v_3^2 + v_1^2 (v_2^2 + 4v_3^2)}.\end{aligned}\tag{24}$$

From the theoretical side we have to ensure that the scalar potential in the model is bounded from below (BFB).

### A. Boundedness Conditions

In order to ensure that the scalar potential in eq. (4) is bounded from below we have to derive the conditions on the dimensionless parameters such the quartic part of the scalar potential is positive  $V^{(4)} > 0$  as the fields go to infinity. We have that the parameter  $\kappa \ll 1$  (due to the smallness of the neutrino mass) and non-negative. This follows from

$$\kappa \approx 2m_A^2 \frac{v_3}{v_1 v_2^2}.\tag{25}$$

where we have used the last expression in eq. (24) and the fact that  $v_3 \ll v_2, v_1$ . Then  $\kappa$  is neglected with respect to the other dimensionless parameters  $\lambda_i$  and  $\beta_j$ , i.e.  $\lambda_i, \beta_j \gg \kappa$ . As a result the quartic part of the potential  $V^{(4)}|_{\kappa=0}$  turns to be a biquadratic form  $\lambda_{ij} \varphi_i^2 \varphi_j^2$  of real fields. Therefore, in this strict limit, the copositivity criteria described in [22] may be applied and the boundedness conditions for eq. (4) are the following,

$$\begin{aligned}\lambda_1 &> 0, \quad \beta_1 > 0, \quad \lambda_{24} > 0, \quad \hat{\lambda} \equiv \beta_2 + 2\sqrt{\beta_1 \lambda_1} > 0, \\ \tilde{\lambda} &\equiv \beta_3 + 2\sqrt{\beta_1 \lambda_{24}} > 0, \quad \bar{\lambda} \equiv \lambda_3 + \theta(-\lambda_5) \lambda_5 + 2\sqrt{\lambda_1 \lambda_{24}} > 0, \quad \text{and} \\ \sqrt{\beta_1 \lambda_1 \lambda_{24}} &+ [\lambda_3 + \theta(-\lambda_5) \lambda_5] \sqrt{\beta_1} + \beta_2 \sqrt{\lambda_{24}} + \beta_3 \sqrt{\lambda_1} + \sqrt{\hat{\lambda} \tilde{\lambda} \bar{\lambda}} > 0,\end{aligned}\tag{26}$$

where  $\lambda_{24} \equiv \lambda_2 + \lambda_4$ . In addition all the dimensionless parameters in the scalar potential are required to be less than  $\sqrt{4\pi}$  in order to fulfill the perturbativity condition.

### B. Astrophysical constraints

In our type-II seesaw model there are some constraints on the magnitude of  $SU(2)$  triplet's vev  $\langle \Delta \rangle = v_3$ , that one must take into account. First of all,  $v_3$  is constrained to be smaller than a few GeVs due to the  $\rho$  parameter (  $\rho = 1.0004 \pm 0.00024$  [23]).

On the other hand, the presence of the Nambu-Goldstone boson associated to spontaneous lepton number violation and neutrino mass generation implies that there is a most stringent constraint on  $v_3$  coming from astrophysics, due to supernova cooling. If the majoron is a strict Goldstone boson (or lighter than typical stellar temperatures) one has an upper bound for the Majoron-electron coupling

$$|g_{Jee}| \lesssim 10^{-13},$$

This is discussed, for example, in Ref. [24] and references therein. This implies

$$|g_{Jee}| = |\mathcal{O}_{12}^I m_e / v_2|.$$

Taking into account the profile of the Majoron [14]<sup>3</sup> one can translate this as a bound on the projection of the Majoron onto the doublet as follows [16]

$$|\langle J | \phi \rangle| = \frac{2|v_2|v_3^2}{\sqrt{v_1^2(v_2^2 + 4v_3^2)^2 + 4v_2^2v_3^4 + v_2^4v_3^2}} \lesssim 10^{-7}. \quad (27)$$

Notice that this restriction on the triplet's vev is stronger than the one stemming from the  $\rho$  parameter. The shaded region in Fig. 2 corresponds to the allowed region of  $v_3$  as function of  $v_1$ .

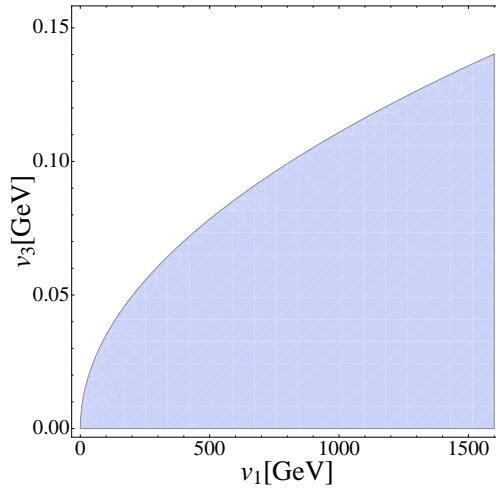


Figure 2: The shaded region represents the allowed region of  $v_3$  as function of  $v_1$ .

To close this section we mention that our phenomenological analysis remains valid if the Nambu-Goldstone boson picks up a small mass from, say, quantum gravity effects.

---

<sup>3</sup> This is derived either by explicit analysis of the scalar potential or simply by symmetry, using Noether's theorem [14].

#### IV. TYPE-II SEESAW HIGGS SEARCHES AT THE LHC

We now turn to the study of the experimental sensitivities of the LHC experiments to the parameters characterizing the “123” type-II majoron seesaw Higgs sector, as proposed in [14]. In the following we will assume that  $m_{H_1} < m_{H_2} < m_{H_3}$  where 1,2,3 refer to the mass ordering in the CP even Higgs sector. Therefore, there are two possible cases that can be considered<sup>4</sup>:

(i)  $m_{H_1} < m_H$  and  $m_{H_2} = m_H$ ;

(ii)  $m_{H_1} = m_H$ ,

where  $m_H$  is the mass of the Higgs reported by the ATLAS [2] and CMS [25] collaborations, i.e.  $m_H = 125.09 \pm 0.21(\text{stat.}) \pm 0.11(\text{syst.})$  GeV [26]. For case (i), we have to enforce the constraints coming from LEP-II data on the lightest CP-even scalar coupling to the SM and those coming from the LHC Run-1 on the heavier scalars. Such situation has been discussed by us in Ref. [13] in the simplest “12-type” seesaw Majoron model. In case (ii), only the constraints coming from the LHC must be taken into account.

The neutral component of the Standard Model Higgs doublet couplings get modified as follows,

$$\phi^0 \rightarrow C_1 H_1 + C_2 H_2 + C_3 H_3 \quad (28)$$

where we have defined  $C_i \equiv \mathcal{O}_{i2}^R$  and  $\mathcal{O}_{ij}^R$  are the matrix elements of  $\mathcal{O}^R$  in eq. (9).

##### A. LEP constraints on invisible Higgs decays

The constraints on  $H_1$ , when  $m_{H_1} < 125$  GeV, stem from the process  $e^+e^- \rightarrow Zh \rightarrow Zb\bar{b}$  which is written as [27]

$$\begin{aligned} \sigma_{hZ \rightarrow b\bar{b}Z} &= \sigma_{hZ}^{SM} \times R_{hZ} \times BR(h \rightarrow b\bar{b}) \\ &= \sigma_{hZ}^{SM} \times C_{Z(h \rightarrow b\bar{b})}^2, \end{aligned} \quad (29)$$

where  $\sigma_{hZ}^{SM}$  is the SM  $hZ$  cross section,  $R_{hZ}$  is the suppression factor related to the coupling of the Higgs boson<sup>5</sup> to the gauge boson  $Z$ . Since  $v_3 \ll v_2$ , we have that the factor  $R_{H_i Z} \approx C_i^2$  where  $C_1 = \cos \alpha_{13} \sin \alpha_{12}$ , eq. (28). Notice that  $C_1 \approx \sin \alpha_{12}$  for the limit  $\alpha_{13} \ll 1$  and then one obtains the same exclusion region depicted in Fig. 1 in Ref. [13].

<sup>4</sup> Recall that  $m_{H_3} \approx m_A$ , eq. (22), which implies that the mass of  $H_3$  must be close to that of the doubly-charged scalar mass. Therefore, as we will see in the next section, the existing bounds on searches of the doubly-charged scalar exclude the case where  $m_{H_3}$  is lighter than the other CP-even mass eigenstates.

<sup>5</sup> The Feynman rules for the couplings of the Higgs bosons  $H_i$  to the  $Z$  are the following:  
 $i \frac{g^2}{2c_W^2} (\mathcal{O}_{i2}^R v_2 + \mathcal{O}_{i3}^R v_3) g_{\mu\nu}$

## B. LHC constraints on the Higgs signal strengths

In addition, we have to enforce the limits coming from the Standard Model decay channels of the Higgs boson. These are given in terms of the signal strength parameters,

$$\mu_f = \frac{\sigma^{\text{NP}}(pp \rightarrow h)}{\sigma^{\text{SM}}(pp \rightarrow h)} \frac{BR^{\text{NP}}(h \rightarrow f)}{BR^{\text{SM}}(h \rightarrow f)}, \quad (30)$$

where  $\sigma$  is the cross section for Higgs production,  $BR(h \rightarrow f)$  is the branching ratio into the Standard Model final state  $f$ , the labels NP and SM stand for New Physics and Standard Model respectively. These can be compared with those given by the experimental collaborations. The most recent results of the signal strengths from a combined ATLAS and CMS analysis [28] are shown in Table I.

channel	ATLAS	CMS	ATLAS+CMS
$\mu_{\gamma\gamma}$	$1.15^{+0.27}_{-0.25}$	$1.12^{+0.25}_{-0.23}$	$1.16^{+0.20}_{-0.18}$
$\mu_{WW}$	$1.23^{+0.23}_{-0.21}$	$0.91^{+0.24}_{-0.21}$	$1.11^{+0.18}_{-0.17}$
$\mu_{ZZ}$	$1.51^{+0.39}_{-0.34}$	$1.05^{+0.32}_{-0.27}$	$1.31^{+0.27}_{-0.24}$
$\mu_{\tau\tau}$	$1.41^{+0.40}_{-0.35}$	$0.89^{+0.31}_{-0.28}$	$1.12^{+0.25}_{-0.23}$
$\mu_{bb}$	$0.62^{+0.37}_{-0.36}$	$0.81^{+0.45}_{-0.42}$	$0.69^{+0.29}_{-0.27}$

Table I: Current experimental results of ATLAS and CMS, Ref. [28].

One can see with ease that the LHC results indicate that  $\mu_{VV} \sim 1$ . In our analysis, we assume that the LHC allows deviations up to 20% as follows,

$$0.8 \leq \mu_{XX} \leq 1.2 \quad (31)$$

## C. LHC bounds on the heavy neutral scalars

In our study we will impose the constraints on the heavy scalars from the recent LHC scalar boson searches. Therefore, we use the bounds set by the search for a heavy Higgs in the  $H \rightarrow WW$  and  $H \rightarrow ZZ$  decay channels in the range  $[145 - 1000]$  GeV [29] and in the  $h \rightarrow \tau\tau$  decay channel in the range  $[100 - 1000]$  GeV [30]. We also adopt the constraints on the process  $h \rightarrow \gamma\gamma$  in the range  $[65 - 600]$  GeV [31] and the range  $[150, 850]$  GeV [32]. Besides, we impose the bounds in the  $A \rightarrow Zh$  decay channel in the range  $[220 - 1000]$  GeV [33].

## D. Summary of the searches of charged scalars

The type-II seesaw model with explicit breaking of lepton number contains seven physical scalars: two CP-even neutral scalars  $H_1$  and  $H_2$ , one CP-odd scalar  $A$  and four charged scalars  $\Delta^{\pm\pm}$  and  $H^\pm$ . Such a scenario has been widely studied in the literature and turns out to be quite appealing because it could be tested at the LHC [34–44]. For instance, the existence of charged scalar bosons provides additional contributions to the one-loop decays of the Standard Model Higgs boson. Indeed, they could affect the one-loop decays  $h \rightarrow \gamma\gamma$  [39, 40] and  $h \rightarrow Z\gamma$  [40] in a substantial way. In this case the signal strength  $\mu_{\gamma\gamma}$  can set bounds on the mass of the charged scalars,  $\Delta^{\pm\pm}$  and/or  $H^\pm$ .

The doubly-charged scalar boson has the following possible decay channels:  $\ell^\pm\ell^\pm$ ,  $W^\pm W^\pm$ ,  $W^\pm H^\pm$  and  $H^\pm H^\pm$ . However, it is known that for an approximately degenerate triplet mass spectrum and vev  $v_3 \lesssim 10^{-4} \text{ GeV}$  the doubly charged Higgs coupling to  $W^\pm$  is suppressed (because it is proportional to  $v_3$  as can be seen from Table III) and hence  $\Delta^{\pm\pm}$  predominantly decays into like-sign dileptons [41, 44, 45]. In this case, CMS [46] and ATLAS [47] have currently excluded at 95% C.L., depending on the assumptions on the branching ratios into like-sign dileptons, doubly-charged masses between 200 and 460 GeV<sup>6</sup>. For  $v_3 \gtrsim 10^{-4} \text{ GeV}$ , the Yukawa couplings of triplet to leptons are too small so that  $\Delta^{\pm\pm}$  dominantly decays to like-sign dibosons, in which case the collider limits are rather weak [43, 48–50].

In the present “123” type-II seesaw model there are two additional physical scalars, a massive CP-even scalar  $H_3$  and the massless majoron  $J$ . The latter, associated to the spontaneous breaking of lepton number, provides non-standard decay channels of other Higgs bosons as missing energy in the final state<sup>7</sup>.

## V. INVISIBLE HIGGS DECAYS AT THE LHC

We now turn to the case of genuinely non-standard Higgs decays. We focus on investigating the LHC sensitivities on the invisible Higgs decays. In so doing we take into account how they are constrained by the available experimental data. In the previous section we mentioned that in our study the CP- even scalars obey the following mass hierarchy  $m_{H_1} < m_{H_2} < m_{H_3}$ . Furthermore, we will also assume that the masses  $m_{H_3}$ ,  $m_A$ ,  $m_{H^\pm}$  and

<sup>6</sup> From doubly-charged scalar boson searches performed by ATLAS and CMS one can also constrain the lepton number violation processes  $pp \rightarrow \Delta^{\pm\pm} \Delta^{\mp\mp} \rightarrow \ell^\pm \ell^\pm W^\mp W^\mp$  and  $pp \rightarrow \Delta^{\pm\pm} H^\mp \rightarrow \ell^\pm \ell^\pm W^\mp Z$  [41]. This may also shed light on the Majorana phases of the lepton mixing matrix [34–36].

<sup>7</sup> These include, for example,  $H_i \rightarrow JJ$  and  $H^\pm \rightarrow JW^\mp$ . Here we focus mainly on the first, the decays of  $H^\pm$  deserve further study but it is beyond the scope of this work and will be considered elsewhere.

$m_{\Delta^{++}}$  are nearly degenerate. As a consequence, the decay of any CP-even Higgs  $H_i$  into the pseudo-scalar  $A$  is not kinematically allowed. Therefore, the new decay channels of the CP-even scalars are just,  $H_i \rightarrow JJ$  and  $H_i \rightarrow 2H_j$  (when  $m_{H_i} < \frac{m_{H_j}}{2}$  for  $i \neq j$ ). The latter contributing also to the invisible decay channel of the Higgs as,  $H_i \rightarrow 2H_j \rightarrow 4J$ .

The Higgs-Majoron couplings are given by,

$$g_{H_a JJ} = \left( \frac{(\mathcal{O}_{12}^I)^2}{v_2} \mathcal{O}_{a2}^R + \frac{(\mathcal{O}_{13}^I)^2}{v_3} \mathcal{O}_{a3}^R + \frac{(\mathcal{O}_{11}^I)^2}{v_1} \mathcal{O}_{a1}^R \right) m_{H_a}^2, \quad (32)$$

where  $\mathcal{O}_{ij}^I$  are the elements of the rotation matrix in eq. (13) and the decay width is given by

$$\Gamma(H_a \rightarrow JJ) = \frac{1}{32\pi} \frac{g_{H_a JJ}^2}{m_{H_a}}. \quad (33)$$

Following our conventions we have that the trilinear coupling  $H_2 H_1 H_1$  turns out to be,

$$\begin{aligned} \frac{g_{H_2 H_1 H_1}}{2} &= 3\lambda_1 (\mathcal{O}_{12}^R)^2 \mathcal{O}_{22}^R v_2 + 3(\lambda_2 + \lambda_4) (\mathcal{O}_{13}^R)^2 \mathcal{O}_{23}^R v_3 \\ &+ \frac{(\lambda_3 + \lambda_5)}{2} \left[ (\mathcal{O}_{13}^R)^2 \mathcal{O}_{22}^R v_2 + (\mathcal{O}_{12}^R)^2 \mathcal{O}_{23}^R v_3 + 2\mathcal{O}_{12}^R \mathcal{O}_{13}^R (\mathcal{O}_{23}^R v_2 + \mathcal{O}_{22}^R v_3) \right] \\ &+ 3\beta_1 (\mathcal{O}_{11}^R)^2 \mathcal{O}_{21}^R v_1 + \frac{\beta_2}{2} \left[ (\mathcal{O}_{12}^R)^2 \mathcal{O}_{21}^R v_1 + (\mathcal{O}_{11}^R)^2 \mathcal{O}_{22}^R v_2 + 2\mathcal{O}_{11}^R \mathcal{O}_{12}^R (\mathcal{O}_{22}^R v_1 + \mathcal{O}_{21}^R v_2) \right] \\ &+ \frac{\beta_3}{2} \left[ (\mathcal{O}_{13}^R)^2 \mathcal{O}_{21}^R v_1 + (\mathcal{O}_{11}^R)^2 \mathcal{O}_{23}^R v_3 + 2\mathcal{O}_{11}^R \mathcal{O}_{13}^R (\mathcal{O}_{23}^R v_1 + \mathcal{O}_{21}^R v_3) \right] \\ &+ \frac{\kappa}{2} \left[ -2\mathcal{O}_{11}^R \mathcal{O}_{13}^R \mathcal{O}_{22}^R v_2 - (\mathcal{O}_{12}^R)^2 (\mathcal{O}_{23}^R v_1 + \mathcal{O}_{21}^R v_3) - 2\mathcal{O}_{12}^R (\mathcal{O}_{13}^R (\mathcal{O}_{22}^R v_1 + \mathcal{O}_{21}^R v_2) \right. \\ &\left. + \mathcal{O}_{11}^R (\mathcal{O}_{23}^R v_2 + \mathcal{O}_{22}^R v_3)) \right]. \end{aligned} \quad (34)$$

and hence, for example when  $m_{H_1} < 2m_{H_2}$ , the decay width  $H_2 \rightarrow H_1 H_1$  is given by

$$\Gamma(H_2 \rightarrow H_1 H_1) = \frac{g_{H_2 H_1 H_1}^2}{32\pi m_{H_2}} \left( 1 - \frac{4m_{H_1}^2}{m_{H_2}^2} \right)^{1/2}. \quad (35)$$

As we already mentioned, a salient feature of adding an isotriplet to the Standard Model is that some *visible* decay channels of the Higgs receive further contributions from the charged scalars, namely the one-loop decays  $h \rightarrow \gamma\gamma$  and  $h \rightarrow Z\gamma$ . That is, the scalars  $H^\pm$  and  $\Delta^{\pm\pm}$  contribute to the one-loop coupling of the Higgs to two-photons and to  $Z$ -photon, leading to deviations from the Standard Model expectations for these decay channels. The interactions between CP-even and charged scalars are described by the following vertices,

$$\begin{aligned} H_a H^+ H^- &: i g_{H_a H^+ H^-} \\ H_a \Delta^{++} \Delta^{--} &: i g_{H_a \Delta^{++} \Delta^{--}} \end{aligned}$$

where

$$\begin{aligned} g_{H_a H^+ H^-} &= \frac{1}{2(v_2^2 + 2v_3^2)} \left[ 8\lambda_1 \mathcal{O}_{a2}^R v_2 v_3^2 + 4(\lambda_2 + \lambda_4) \mathcal{O}_{a3}^R v_2^2 v_3 + 2\lambda_3 (\mathcal{O}_{a2}^R v_2^3 + 2\mathcal{O}_{a3}^R v_3^3) \right. \\ &+ \lambda_5 v_2 [-2\mathcal{O}_{a3}^R v_2 v_3 + \mathcal{O}_{a2}^R (v_2^2 - 2v_3^2)] + 4\beta_2 \mathcal{O}_{a1}^R v_1 v_3^2 + 2\beta_3 \mathcal{O}_{a1}^R v_1 v_2^2 \\ &\left. + 4\kappa v_2 v_3 (\mathcal{O}_{a2}^R v_1 + \mathcal{O}_{a1}^R v_2) \right] \\ g_{H_a \Delta^{++} \Delta^{--}} &= 2\lambda_2 \mathcal{O}_{a3}^R v_3 + \lambda_3 \mathcal{O}_{a2}^R v_2 + \beta_3 \mathcal{O}_{a1}^R v_1. \end{aligned}$$

Note that the contributions of  $H^\pm$  and  $\Delta^{\pm\pm}$  to the decays  $h \rightarrow \gamma\gamma$  and  $h \rightarrow Z\gamma$  are functions of the singlet's vev  $v_1$ , this is in contrast to what happens in the type-II seesaw model with explicit violation of lepton number. According to eq. (26) the dimensionless parameters  $\lambda_i$  and  $\beta_i$  can change the sign of the couplings of  $g_{H_a H^+ H^-}$  and  $g_{H_a \Delta^{++} \Delta^{--}}$ , hence the contribution of the charged scalars to  $h \rightarrow \gamma\gamma$  and  $h \rightarrow Z\gamma$  may be either constructive or destructive.

For the computation of the decay widths  $h \rightarrow \gamma\gamma$  and  $h \rightarrow Z\gamma$  we use the expressions and conventions given in Ref. [51]. The decay width  $\Gamma(H_a \rightarrow \gamma\gamma)$  turns out to be

$$\Gamma(H_a \rightarrow \gamma\gamma) = \frac{G_F \alpha^2 m_{H_a}^3}{128 \sqrt{2} \pi^3} |X_F^{\gamma\gamma} + X_W^{\gamma\gamma} + X_H^{\gamma\gamma}|^2 \quad (36)$$

where  $G_F$  is the Fermi constant,  $\alpha$  is the fine structure constant and the form factors  $X_i^j$  are given by <sup>8</sup>,

$$\begin{aligned} X_F^{\gamma\gamma} &= -2C_a \sum_f N_c^f Q_f^2 \tau_f [1 + (1 - \tau_f) f(\tau_f)], \\ X_W^{\gamma\gamma} &= C_a [2 + \tau_W + 3\tau_W(2 - \tau_W) f(\tau_W)] \\ X_H^{\gamma\gamma} &= -\frac{g_{H_a H^+ H^-} v}{2m_{H^\pm}^2} \tau_{H^\pm} [1 - \tau_{H^\pm} f(\tau_{H^\pm})] - 4 \frac{g_{H_a \Delta^{++} \Delta^{--}} v}{2m_{\Delta^{\pm\pm}}^2} \tau_{\Delta^{\pm\pm}} [1 - \tau_{\Delta^{\pm\pm}} f(\tau_{\Delta^{\pm\pm}})]. \end{aligned} \quad (37)$$

where  $\tau_x = 4m_x^2/m_Z^2$ . Here  $N_c^F$  and  $Q_F$  denote, respectively, the number of colors and electric charge of a given fermion. The one-loop function  $f(\tau)$  is defined in appendix B. The parameters  $C_a$  correspond to the Standard Model Higgs couplings in eq. (28).

The decay width  $\Gamma(H_a \rightarrow Z\gamma)$ , using the notation in Ref. [51], is expressed as follows

$$\Gamma(H_a \rightarrow Z\gamma) = \frac{G_F \alpha^2 m_{H_a}^3}{64 \sqrt{2} \pi^3} \left(1 - \frac{m_Z^2}{m_{H_a}^2}\right)^3 |X_F^{Z\gamma} + X_W^{Z\gamma} + X_H^{Z\gamma}|^2 \quad (38)$$

---

<sup>8</sup> We have taken into account that  $v_3$  is very small so that any contribution involving the triplet's vev is neglected. Then for instance the Feynman rule for the vertex  $H_a W_\mu^+ W_\nu^- : i \frac{g^2}{2} (O_{a2}^R v_2 + 2O_{a3}^R v_3) g_{\mu\nu}$ , is approximated as  $\sim i \frac{g^2}{2} (O_{a2}^R v_2) g_{\mu\nu}$  (see Table III).

where the form factors  $X_i^j$  are given by<sup>9</sup>,

$$\begin{aligned}
X_F^{Z\gamma} &= -4C_a \sum_f N_c^f \frac{g_V^f Q_f m_f^2}{s_W c_W} \left\{ \frac{2m_Z^2}{(m_{H_a}^2 - m_Z^2)^2} \Delta B_0^f + \frac{1}{m_{H_a}^2 - m_Z^2} \right. \\
&\quad \left. \times \left[ (4m_f^2 - m_{H_a}^2 + m_Z^2) C_0^f + 2 \right] \right\} \\
X_W^{Z\gamma} &= \frac{C_a}{\tan \theta_W} \left\{ \frac{1}{(m_{H_a}^2 - m_Z^2)^2} \left[ m_{H_a}^2 (1 - \tan^2 \theta_W) - 2m_W^2 (-5 + \tan^2 \theta_W) \right] m_Z^2 \Delta B_0^W \right. \\
&\quad + \frac{1}{(m_{H_a}^2 - m_Z^2)} \left[ m_{H_a}^2 (1 - \tan^2 \theta_W) - 2m_W^2 (-5 + \tan^2 \theta_W) \right. \\
&\quad \left. \left. + 2m_W^2 \left[ (-5 + \tan^2 \theta_W)(m_{H_a}^2 - 2m_W^2) - 2m_Z^2 (-3 + \tan^2 \theta_W) \right] C_0^W \right] \right\} \\
X_H^{Z\gamma} &= -2g_{H_a H^+ H^-} v \frac{\tan \theta_W}{(m_{H_a}^2 - m_Z^2)} \left[ \frac{m_Z^2}{m_{H_a}^2 - m_Z^2} \Delta B_0^\pm + (2m_{H^\pm}^2 C_0^\pm + 1) \right] \\
&\quad - 4 \frac{g_{H_a \Delta^{++} \Delta^{--}}}{\tan \theta_W} \frac{(1 - \tan^2 \theta_W)}{(m_{H_a}^2 - m_Z^2)} \left[ \frac{m_Z^2}{m_{H_a}^2 - m_Z^2} \Delta B_0^{\pm\pm} + (2m_{\Delta^{\pm\pm}}^2 C_0^{\pm\pm} + 1) \right]
\end{aligned}$$

where  $C_0^b$  and  $\Delta B_0^b$  are defined in appendix B.

## VI. TYPE-II SEESAW NEUTRAL HIGGS SEARCHES AT THE LHC

We stated above that in our study we are assuming  $m_{H_1} < m_{H_2} < m_{H_3}$  and  $v_1 \gtrsim v_2$ . Furthermore, because of the  $\rho$  parameter and the astrophysical constraint on the triplet's vev we also have that  $v_3 \ll v_1, v_2$ . We found that the smallness of  $v_3$  and the perturbativity condition of the potential lead to a very small mixing between the mass eigenstate  $H_3$  and the CP-even components of the fields,  $\sigma$  and  $\Phi$ , in other words, the angles  $\alpha_{13}$  and  $\alpha_{23}$  must lie close to 0 or  $\pi$ . As a result, we obtain the following relation,

$$m_{H_3}^2 - m_A^2 \simeq 2\lambda_2 v_3^2 \implies m_{H_3} \simeq m_A. \quad (39)$$

This extra mass relation is derived from eq. (24), by using eq. (25) and the fact that  $\alpha_{13,23} \sim 0(\pi)$ . In addition, also as a result of  $\alpha_{13,23} \sim 0(\pi)$ , we find that the coupling of  $H_3$  to the Standard Model states is negligible,

$$\frac{g_{H_3 ff}}{g_{hff}^{\text{SM}}} = \frac{g_{H_3 VV}}{g_{hVV}^{\text{SM}}} = C_3 \sim 0. \quad (40)$$

In Fig. 12 of appendix A we give a schematic illustration of the mass profile of the Higgs bosons in our model. The mass spectrum and composition are summarized in Table II, and provide a useful picture in our following analyses.

### A. Analysis (i)

In this case we have taken the isotriplet vev  $v_3 = 10^{-5}$  GeV, automatically safe from the constraints stemming from astrophysics and the  $\rho$  parameter. We have also considered

<sup>9</sup> Here we have also assumed  $v_3 \ll 1$  so as to make the following approximation,  $H^+ H^- Z_\mu : -ig \sin \theta_W \tan \theta_W (p_+ - p_-)_\mu$ .

the following mass spectrum,

$$m_{H_1} = [15, 115] \text{ GeV}, \quad m_{H_2} = 125 \text{ GeV}, \quad m_{H_3} \simeq m_A \simeq m_{H^\pm} \simeq m_{\Delta^{\pm\pm}} = 500 \text{ GeV},$$

and varied the parameters as

$$v_1 \in [100, 2500] \text{ GeV}, \quad \alpha_{12} \in [0, \pi] \quad \text{and} \quad \alpha_{13,23} = \delta_\alpha (\pi - \delta_\alpha) \quad (41)$$

where  $0 \leq \delta_\alpha < 0.1$ . As described in section IV we must enforce the LEP constraints on the lightest CP-even Higgs  $H_1$  and LHC constraints on the heavier scalars. The near mass degeneracy of  $H_3$ ,  $A$ ,  $H^\pm$  and  $\Delta^{\pm\pm}$  ensures that the oblique parameters are not affected. In analogy to the type-II seesaw model with explicit lepton number violation we expect that, because of  $v_3 < 10^{-4} \text{ GeV}$ , the doubly-charged scalar predominantly decays into same sign dileptons [41, 44, 45] and that  $m_{\Delta^{\pm\pm}} = 500 \text{ GeV}$  is consistent with current experimental data, see subsection IV D.

We show in Fig. 3 the mass of the lightest CP-even scalar as a function of the absolute value of its coupling to the Standard Model states,  $|C_1|$  in eq. (28). The blue region corresponds to the LEP exclusion region and the green(red) one is the LHC allowed(exclusion) region provided by the signal strengths  $0.8 < \mu_{XX} < 1.2$ .

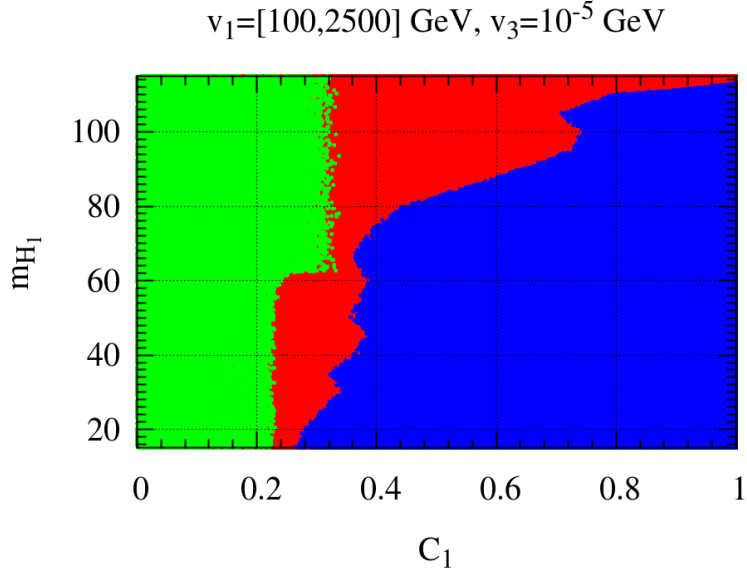


Figure 3: Analysis (i). The mass of the lightest CP-even scalar as a function of the absolute value of its coupling to Standard Model states. The blue region corresponds to the LEP exclusion region and the green(red) one is the LHC allowed(exclusion) region.

The presence of light charged scalars can enhance significantly the diphoton channel of the Higgs [39]. Fig. 4 shows the correlation between  $\mu_{ZZ}$  and  $\mu_{\gamma\gamma}(\mu_{Z\gamma})$  on the left(right)

with  $\mu_{\gamma\gamma} \lesssim 1.2$  for charged Higgs bosons of 500 GeV. The correlation between the signal strength  $\mu_{ZZ}$  and the signal strengths  $\mu_{\gamma\gamma}$  and  $\mu_{Z\gamma}$  is shown in Fig. 4. Note that the former may exceed one due to the new contributions of the singly and doubly charged Higgs bosons.

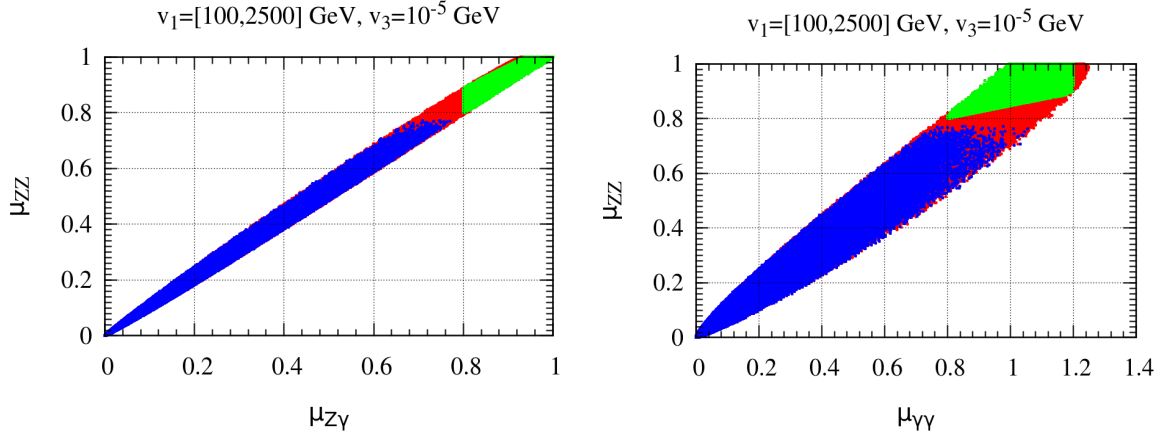


Figure 4: Analysis (i). On the left, we show correlation between  $\mu_{ZZ}$  and  $\mu_{Z\gamma}$ . On the right, correlation between  $\mu_{ZZ}$  and  $\mu_{\gamma\gamma}$ . The color code as in Fig. 3.

The invisible decays of the Higgs bosons, characteristic of the model, turn out to be correlated to the visible channels, represented in terms of the signal strengths, as shown in Fig. 5. Note that the upper bound on the invisible decays of a Higgs boson with a mass of 125 GeV has been found to be  $\text{BR}(H_2 \rightarrow \text{Inv}) \lesssim 0.2$ . This limit is stronger than those provided by the ATLAS [52] and the CMS [53] collaborations<sup>10</sup>.

In Fig. 6 we depict the correlation between the invisible branching ratios of  $H_2$  with the one of the lightest scalar boson  $H_1$ . And, as can be seen,  $H_1$  can decay 100% into the invisible channel (majorons).

<sup>10</sup> The ATLAS collaboration has set an upper bound on the  $\text{BR}(H \rightarrow \text{Inv})$  at 0.28 while the CMS collaboration reported that the observed (expected) upper limit on the invisible branching ratio is 0.58(0.44), both results at 95% C.L.

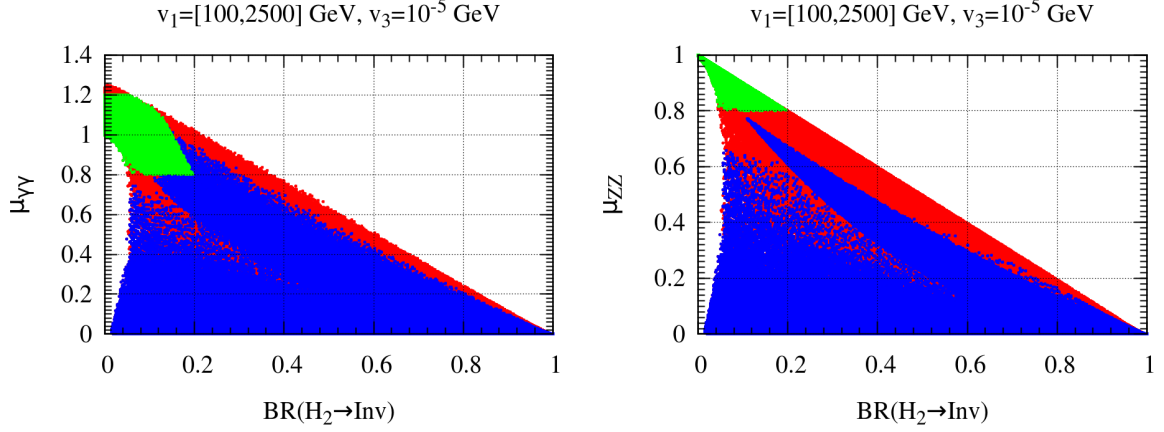


Figure 5: Analysis (i). On the left: the signal strength  $\mu_{\gamma\gamma}$  versus  $\text{BR}(H_2 \rightarrow \text{Inv})$ . On the right:  $\mu_{ZZ}$  versus  $\text{BR}(H_2 \rightarrow \text{Inv})$ . The color code as in Fig. 3.

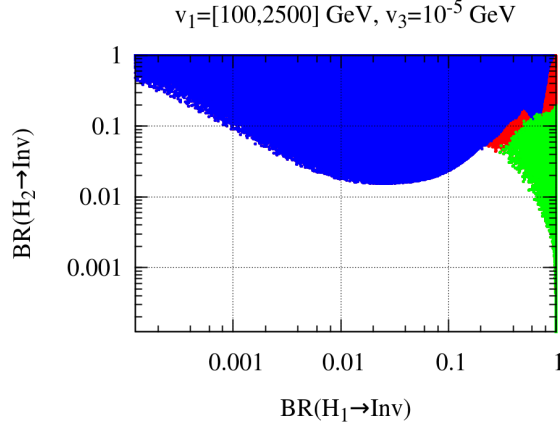


Figure 6: Analysis (i). Correlation between the invisible branchings  $\text{BR}(H_2 \rightarrow \text{Inv})$  and  $\text{BR}(H_1 \rightarrow \text{Inv})$ . The color code as in Fig. 3.

Finally, as we have mentioned we obtained that the reduced coupling of  $H_3$  to the Standard Model states is  $C_3 \sim \mathcal{O}(10^{-7})$  so that it is basically decoupled. As a result its invisible branching is essentially unconstrained,  $10^{-5} \lesssim \text{BR}(H_3 \rightarrow \text{Inv}) \leq 1$ . On the other hand we find that the constraint coming from the LHC on the pseudo-scalar  $A$  with a mass of 500 GeV is automatically satisfied as well, since from the LHC,  $\sigma(gg \rightarrow A)\text{BR}(A \rightarrow ZH_2)\text{BR}(H_2 \rightarrow \tau\tau) \lesssim 10^{-2}$  while for  $m_A = 500$  GeV we obtain  $\sigma(gg \rightarrow A)\text{BR}(A \rightarrow ZH_2)\text{BR}(H_2 \rightarrow \tau\tau) \lesssim 10^{-15}$ .

## B. Analysis (ii)

We now turn to the other case of interest, namely

$$m_{H_1} = 125 \text{ GeV}, \quad m_{H_2} = [150, 500] \text{ GeV}, \quad m_{H_3} \simeq m_A \simeq m_{H^\pm} \simeq m_{\Delta^{\pm\pm}} = 600 \text{ GeV},$$

with  $v_3 = 10^{-5}$  GeV, as before. Now we scanned over

$$v_1 \in [100, 2500] \text{ GeV}, \quad \alpha_{12} \in [0, \pi] \quad \text{and} \quad \alpha_{13,23} = \delta_\alpha (\pi - \delta_\alpha) \quad (42)$$

where  $0 \leq \delta_\alpha < 0.1$ . As we already mentioned in this case we only have to take into account the constraints coming from Run 1 of the LHC at 8 TeV, see Table I. In practice we assume  $\mu_{XX} = 1.0^{+0.2}_{-0.2}$ . We show in Fig. 7 the correlation between  $\mu_{ZZ}$  and  $\mu_{\gamma\gamma}(\mu_{Z\gamma})$  on the left(right). As before, the allowed region is in green while the forbidden one is in red. We can see that  $\mu_{\gamma\gamma} \lesssim 1.2$  for  $m_{H^\pm} \simeq m_{\Delta^{\pm\pm}} = 600$  GeV.

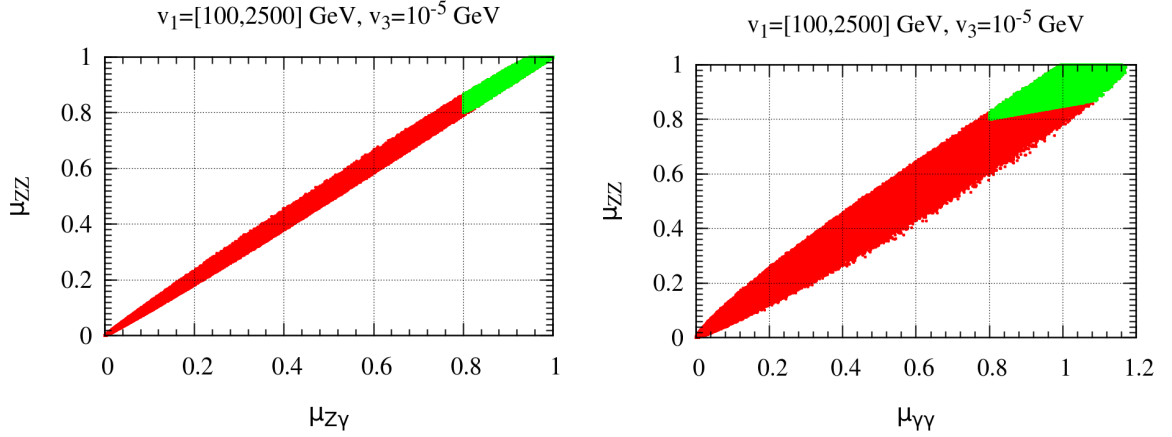


Figure 7: Analysis (ii). On the left,  $\mu_{ZZ}$  versus  $\mu_{Z\gamma}$ . On the right,  $\mu_{ZZ}$  versus  $\mu_{\gamma\gamma}$ . The allowed region (in green) is the region inside the range  $\mu_{XX} = 1.0^{+0.2}_{-0.2}$  while the forbidden one (in red) is the one outside that range.

On the left(right) of Fig. 8 is depicted the correlation between the signal strength  $\mu_{ZZ}$  ( $\mu_{\gamma\gamma}$ ) and the branching ratio of the channel  $H_1 \rightarrow JJ$ . We can see in Figs. 8-10 that  $\text{BR}(H_1 \rightarrow \text{Inv}) \lesssim 0.2$ . One can see from Fig. 9 that  $\text{BR}(H_1 \rightarrow \text{Inv}) \lesssim 0.1$  for  $v_1 \gtrsim 2500$  GeV.

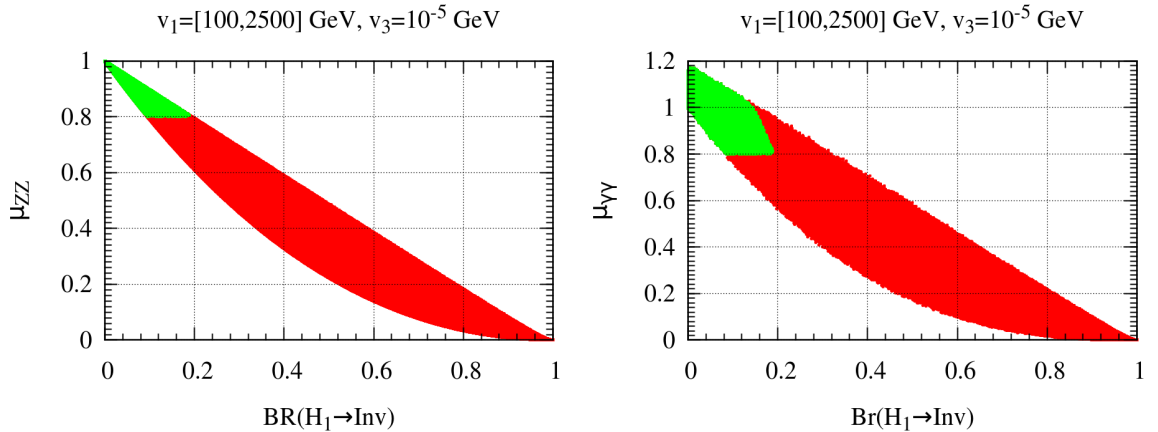


Figure 8: Analysis (ii). On the left: the signal strength  $\mu_{ZZ}$  versus  $\text{BR}(H_1 \rightarrow \text{Inv})$ . On the right:  $\mu_{\gamma\gamma}$  versus  $\text{BR}(H_1 \rightarrow \text{Inv})$ . The color code as in Fig. 7

In this case we find that eq. 32 (for  $\alpha_{13,23} \sim 0(\pi)$  and  $v_3 \ll v_1, v_2$ ) at leading order is given by,

$$g_{H_1 JJ} \sim \frac{\cos \alpha_{12}}{v_1} m_{H_1}^2, \quad (43)$$

where  $m_{H_1} = 125 \text{ GeV}$ .  $\text{BR}(H_1 \rightarrow \text{Inv})$  versus the Higgs-majoron coupling  $g_{H_1 JJ}$  is shown on the right of Fig. 9. Note also from the left panel in Fig. 9 that  $\text{BR}(H_1 \rightarrow \text{Inv})$  is anti-correlated with  $v_1$ , as expected.

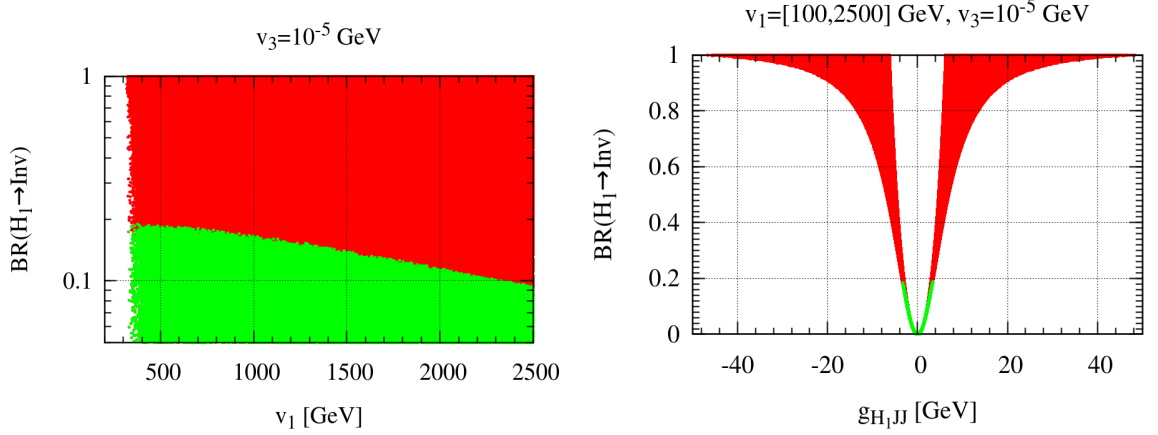


Figure 9: Analysis (ii).  $\text{BR}(H_1 \rightarrow \text{Inv})$  versus  $v_1$  (on the left) and  $\text{BR}(H_1 \rightarrow \text{Inv})$  versus the Higgs-majoron coupling  $g_{H_1 JJ}$  (on the right). The color code as in Fig. 7.

In Fig. 10 we show the correlation between the invisible branching ratio of  $H_2$  (the Higgs with a mass in the range  $150 \text{ GeV} < m_{H_2} < 500 \text{ GeV}$ ) and the one of  $H_1$ .

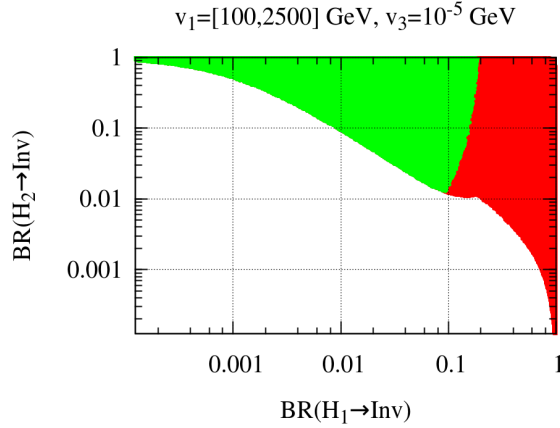


Figure 10: Analysis (ii). Correlation between  $\text{BR}(H_2 \rightarrow \text{Inv})$  and  $\text{BR}(H_1 \rightarrow \text{Inv})$ . The color code as in Fig. 7.

We have verified that the LHC constraints on the heavy scalars ( $H_2$ ,  $H_3$  and  $A$ ) are all satisfied. As an example, the reader can convince her/himself by looking at Fig. 11 that  $H_2$  easily passes the restriction stemming from  $\sigma(ggH_2)\text{BR}(H_2 \rightarrow \tau\tau)$  (top left) and/or

$\sigma(bbH_2)BR(H_2 \rightarrow \tau\tau)$  (top right). The black continuous lines on those plots represent the experimental results from Run 1 of the CMS experiment [30]. We also found that the square of the reduced coupling of  $H_2$  to the Standard Model states is  $C_2^2 \lesssim 0.1$  for  $m_{H_2} = [150, 500]$  GeV. Then, one finds that the experimental upper bounds set by the search for a heavy Higgs in the  $H \rightarrow WW$  and  $H \rightarrow ZZ$  decay channels in [3, 29] are automatically fulfilled. However, improved sensitivities expected from Run 2 may provide a meaningful probe of the theoretically consistent region, depicted in green.

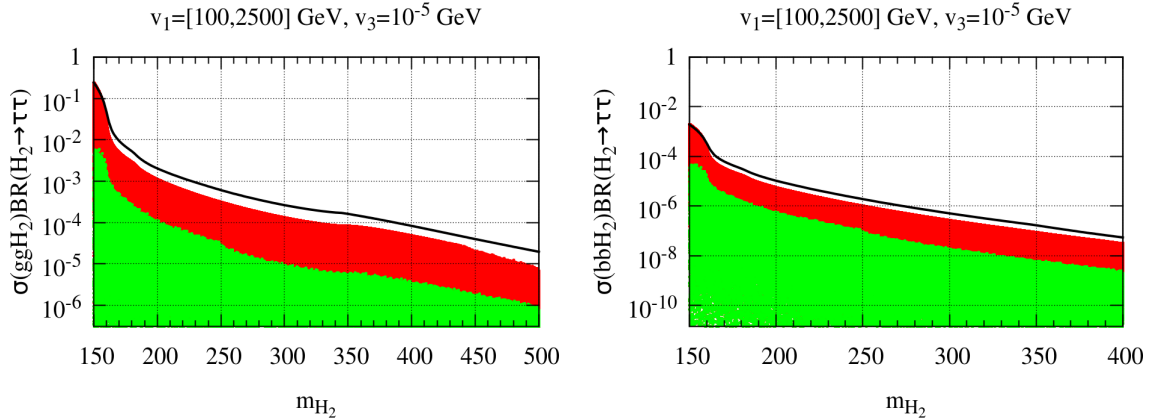


Figure 11: Analysis (ii). On the top right (left)  $\sigma(ggH_2)BR(H_2 \rightarrow \tau\tau)$  ( $\sigma(bbH_2)BR(H_2 \rightarrow \tau\tau)$ ) versus the mass of  $H_2$ .

Also in this case,  $H_3$  is decoupled, so the restrictions on  $H_3$  and the massive pseudoscalar  $A$  are automatically fulfilled.

## VII. CONCLUSIONS

In this paper we have presented the main features of the electroweak symmetry breaking sector of the simplest type-II seesaw model with spontaneous violation of lepton number. The Higgs sector has two characteristic features: a) the existence of a (nearly) massless Nambu-Goldstone boson and b) all neutral CP-even and CP-odd, as well as singly and doubly-charged scalar bosons coming mainly from the triplet are very close in mass, as illustrated in Fig. 12 of appendix A. However, one extra CP-even state, namely  $H_2$  coming from a doublet-singlet mixture can be light. After reviewing the “theoretical” and experimental restrictions which apply on the Higgs sector, we have studied the sensitivities of the searches for Higgs bosons at the ongoing ATLAS/CMS experiments, including not only the new contributions to Standard Model decay channels, but also the novel Higgs decays to majorons. For these we have considered two cases, when the 125 GeV state found at CERN is either (i) the second-to-lightest or (ii) the lightest CP-even scalar boson. For case (i), we have enforced the constraints coming from LEP-II data on the lightest CP-even scalar coupling to the Standard Model states and those coming from the LHC Run-1 on the

heavier scalars. In case (ii), only the constraints coming from the LHC must be taken into account. Such “invisible” Higgs boson decays give rise to missing momentum events. We have found that the experimental results from Run 1 on the search for a heavy Higgs in the  $H \rightarrow WW$  and  $H \rightarrow ZZ$  decay channels are automatically fulfilled. However, improved sensitivities expected from Run 2 may provide a meaningful probe of this scenario. In short we have discussed how the neutrino mass generation scenario not only suggests the need to reconsider the physics of electroweak symmetry breaking from a new perspective, but also provides a new theoretically consistent and experimentally viable paradigm.

## VIII. ACKNOWLEDGMENTS

Work supported by the Spanish grants FPA2014-58183-P, Multidark CSD2009-00064 and SEV-2014-0398 (MINECO), and PROMETEOII/2014/084 (Generalitat Valenciana). C. B. thanks Departamento de Física and CFTP, Instituto Superior Técnico, Universidade de Lisboa, for its hospitality while part of this work was carried out. J.C.R. is also support in part by the Portuguese Fundação para a Ciência e Tecnologia (FCT) under contracts UID/FIS/00777/2013 and CERN/FIS-NUC/0010/2015, which are partially funded through POCTI (FEDER), COMPETE, QREN and the EU.

## Appendix A: Higgs boson mass spectrum

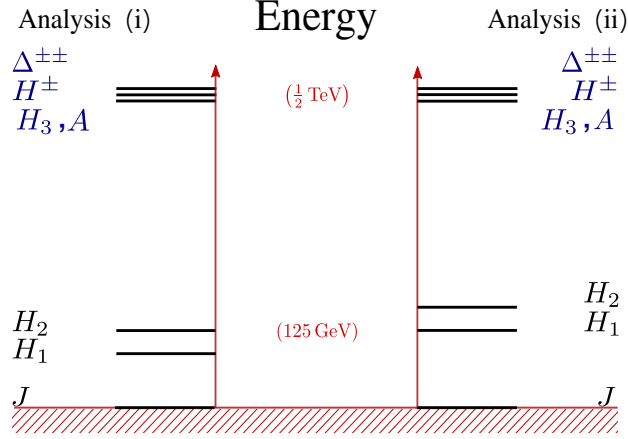


Figure 12: Type-II seesaw Higgs boson mass spectrum

Mass eigenstate $\phi$	Mass squared $m_\phi^2$	Composition
$H_i (i = 1, 2, 3)$	$m_i^2$	$\mathcal{O}_{i1}^R R_1 + \mathcal{O}_{i2}^R R_2 + \mathcal{O}_{i3}^R R_3$
$J$	0	$\mathcal{O}_{11}^I I_1 + \mathcal{O}_{12}^I I_2 + \mathcal{O}_{13}^I I_3$
$G^0$	0	$\mathcal{O}_{22}^I I_2 + \mathcal{O}_{23}^I I_3$
$A$	$\kappa \left( \frac{v_2^2 v_1^2 + v_2^2 v_3^2 + 4v_3^2 v_1^2}{2v_3 v_1} \right)$	$\mathcal{O}_{31}^I I_1 + \mathcal{O}_{32}^I I_2 + \mathcal{O}_{33}^I I_3$
$G^\pm$	0	$c_\pm \phi^\pm + s_\pm \Delta^\pm$
$H^\pm$	$\frac{1}{4v_3} (2\kappa v_1 - \lambda_5 v_3)(v_2^2 + 2v_3^2)$	$-s_\pm \phi^\pm + c_\pm \Delta^\pm$
$\Delta^{\pm\pm}$	$\frac{1}{2v_3} (\kappa v_1 v_2^2 - 2\lambda_4 v_3^3 - \lambda_5 v_2^2 v_3)$	$\Delta^{\pm\pm}$

Table II: Scalar mass eigenstates in the model.  $c_\pm = v_2 / \sqrt{v_2^2 + 2v_3^2}$ ,  $s_\pm = \sqrt{2}v_3 / \sqrt{v_2^2 + 2v_3^2}$

## Appendix B: Loop functions

The one-loop function  $f(\tau)$  used in eq. (37) is given by,

$$f(\tau) = \begin{cases} \arcsin^2(1/\sqrt{\tau}) & \text{if } \tau \geq 1 \\ -\frac{1}{4} \left[ \log \left( \frac{1+\sqrt{1-\tau}}{1-\sqrt{1-\tau}} \right) - i\pi \right]^2 & \text{if } \tau < 1 \end{cases} \quad (\text{B1})$$

The functions  $C_0^b$  and  $\Delta B_0^b$  are given in terms of the Passarino-Veltman functions [54],

$$\begin{aligned} C_0^b &= C_0(m_Z^2, 0, m_{H_a}^2, m_b^2, m_b^2, m_b^2) = -\frac{1}{m_b^2} I_2(\tau_b, \lambda_b), \\ \Delta B_0^b &= B_0(m_{H_a}^2, m_b^2, m_b^2) - B_0(m_Z^2, m_b^2, m_b^2) \\ &= -\frac{m_{H_a}^2 - m_Z^2}{m_Z^2} - \frac{(m_{H_a}^2 - m_Z^2)^2}{2m_a^2 m_Z^2} I_1(\tau_b, \lambda_b) + 2\frac{m_{H_a}^2 - m_Z^2}{m_Z^2} I_2(\tau_b, \lambda_b) \end{aligned} \quad (\text{B2})$$

where  $\lambda_b = 4m_b^2/m_{H_a}^2$ ,

$$\begin{aligned} I_1(\tau, \lambda) &= \frac{\tau\lambda}{2(\tau - \lambda)} + \frac{\tau^2\lambda^2}{2(\tau - \lambda)^2} [f(\tau) - f(\lambda)] + \frac{\tau^2\lambda}{(\tau - \lambda)^2} [g(\tau) - g(\lambda)], \\ I_2(\tau, \lambda) &= -\frac{\tau\lambda}{2(\tau - \lambda)} [f(\tau) - f(\lambda)], \end{aligned} \quad (\text{B3})$$

and

$$g(\tau) = \begin{cases} \sqrt{\tau - 1} \arcsin \sqrt{\tau} & \text{for } \tau \geq 1 \\ \frac{1}{2} \sqrt{1 - \tau} \left( \log \frac{1+\sqrt{1-\tau}}{1-\sqrt{1-\tau}} - i\pi \right) & \text{if } \tau < 1 \end{cases} \quad (\text{B4})$$

## Appendix C: Higgs boson couplings

	Vertex	Gauge Coupling
1	$H_1 W_\mu^+ W_\nu^-$	$i \frac{g^2}{2} (\mathcal{O}_{12}^R v_2 + 2\mathcal{O}_{13}^R v_3) g_{\mu\nu}$
2	$H_2 W_\mu^+ W_\nu^-$	$i \frac{g^2}{2} (\mathcal{O}_{22}^R v_2 + 2\mathcal{O}_{23}^R v_3) g_{\mu\nu}$
3	$H_3 W_\mu^+ W_\nu^-$	$i \frac{g^2}{2} (\mathcal{O}_{32}^R v_2 + 2\mathcal{O}_{33}^R v_3) g_{\mu\nu}$
4	$\Delta^{\pm\pm} W_\mu^\mp W_\nu^\mp$	$i 2g^2 \frac{v_3}{\sqrt{2}} g_{\mu\nu}$
5	$H^\pm W_\mu^\mp Z_\nu$	$i \frac{g^2}{c_W} \frac{c_\pm v_3}{\sqrt{2}} g_{\mu\nu}$
6	$G^\pm W_\mu^\mp Z_\nu$	$i \frac{g^2}{c_W} \left( \frac{v_2}{2} s_W^2 c_\pm + \frac{v_3}{\sqrt{2}} (1 + s_W^2) s_\pm \right) g_{\mu\nu}$
7	$G^\pm W_\mu^\mp A_\nu$	$-i e m_W g_{\mu\nu}$
8	$\Delta^{++} \Delta^{--} W_\mu^+ W_\nu^-$	$i g^2 g_{\mu\nu}$
9	$H^+ H^- W_\mu^+ W_\nu^-$	$i \frac{g^2}{2} (1 + 3c_\pm^2) g_{\mu\nu}$
10	$G^+ G^- W_\mu^+ W_\nu^-$	$i \frac{g^2}{2} (1 + 3s_\pm^2) g_{\mu\nu}$
11	$H_1 H_1 W_\mu^+ W_\nu^-$	$i \frac{g^2}{2} (\mathcal{O}_{12}^{R2} + 2\mathcal{O}_{13}^{R2}) g_{\mu\nu}$
12	$H_2 H_2 W_\mu^+ W_\nu^-$	$i \frac{g^2}{2} (\mathcal{O}_{22}^{R2} + 2\mathcal{O}_{23}^{R2}) g_{\mu\nu}$
13	$H_3 H_3 W_\mu^+ W_\nu^-$	$i \frac{g^2}{2} (\mathcal{O}_{32}^{R2} + 2\mathcal{O}_{33}^{R2}) g_{\mu\nu}$
14	$J J W_\mu^+ W_\nu^-$	$i \frac{g^2}{2} (\mathcal{O}_{12}^{I2} + 2\mathcal{O}_{13}^{I2}) g_{\mu\nu}$
15	$G^0 G^0 W_\mu^+ W_\nu^-$	$i \frac{g^2}{2} (\mathcal{O}_{22}^{I2} + 2\mathcal{O}_{23}^{I2}) g_{\mu\nu}$
16	$A A W_\mu^+ W_\nu^-$	$i \frac{g^2}{2} (\mathcal{O}_{32}^{I2} + 2\mathcal{O}_{33}^{I2}) g_{\mu\nu}$
17	$\Delta^{\pm\pm} H^\mp W_\mu^\mp$	$\mp i g c_\pm (p_1 - p_2)_\mu$
18	$\Delta^{\pm\pm} G^\mp W_\mu^\mp$	$\mp i g s_\pm (p_1 - p_2)_\mu$
19	$H_1 H^\pm W_\mu^\mp$	$\pm i \frac{g}{2} (s_\pm \mathcal{O}_{12}^R - \sqrt{2} c_\pm \mathcal{O}_{13}^R) (p_1 - p_2)_\mu$
20	$H_2 H^\pm W_\mu^\mp$	$\pm i \frac{g}{2} (s_\pm \mathcal{O}_{22}^R - \sqrt{2} c_\pm \mathcal{O}_{23}^R) (p_1 - p_2)_\mu$
21	$H_3 H^\pm W_\mu^\mp$	$\pm i \frac{g}{2} (s_\pm \mathcal{O}_{32}^R - \sqrt{2} c_\pm \mathcal{O}_{33}^R) (p_1 - p_2)_\mu$
22	$H^\pm J W_\mu^\mp$	$\frac{g}{2} (s_\pm \mathcal{O}_{12}^I + \sqrt{2} c_\pm \mathcal{O}_{13}^I) (p_1 - p_2)_\mu$
23	$G^0 H^\pm W_\mu^\mp$	$-\frac{g}{2} (s_\pm \mathcal{O}_{22}^I + \sqrt{2} c_\pm \mathcal{O}_{23}^I) (p_1 - p_2)_\mu$
24	$A H^\pm W_\mu^\mp$	$-\frac{g}{2} (s_\pm \mathcal{O}_{32}^I + \sqrt{2} c_\pm \mathcal{O}_{33}^I) (p_1 - p_2)_\mu$
25	$G^\pm H_1 W_\mu^\mp$	$\pm i \frac{g}{2} (c_\pm \mathcal{O}_{12}^R + \sqrt{2} s_\pm \mathcal{O}_{13}^R) (p_1 - p_2)_\mu$
26	$G^\pm H_2 W_\mu^\mp$	$\pm i \frac{g}{2} (c_\pm \mathcal{O}_{22}^R + \sqrt{2} s_\pm \mathcal{O}_{23}^R) (p_1 - p_2)_\mu$
27	$G^\pm H_3 W_\mu^\mp$	$\pm i \frac{g}{2} (c_\pm \mathcal{O}_{32}^R + \sqrt{2} s_\pm \mathcal{O}_{33}^R) (p_1 - p_2)_\mu$
28	$G^\pm J W_\mu^\mp$	$-\frac{g}{2} (c_\pm \mathcal{O}_{12}^I - \sqrt{2} s_\pm \mathcal{O}_{13}^I) (p_1 - p_2)_\mu$
29	$G^0 G^\pm W_\mu^\mp$	$\frac{g}{2} (c_\pm \mathcal{O}_{22}^I - \sqrt{2} s_\pm \mathcal{O}_{23}^I) (p_1 - p_2)_\mu$
30	$A G^\pm W_\mu^\mp$	$\frac{g}{2} (c_\pm \mathcal{O}_{32}^I - \sqrt{2} s_\pm \mathcal{O}_{33}^I) (p_1 - p_2)_\mu$

	Vertex	Gauge Coupling
31	$H_1 Z_\mu Z_\nu$	$i \frac{g^2}{2c_W^2} (\mathcal{O}_{12}^R v_2 + 4\mathcal{O}_{13}^R v_3) g_{\mu\nu}$
32	$H_2 Z_\mu Z_\nu$	$i \frac{g^2}{2c_W^2} (\mathcal{O}_{22}^R v_2 + 4\mathcal{O}_{23}^R v_3) g_{\mu\nu}$
33	$H_3 Z_\mu Z_\nu$	$i \frac{g^2}{2c_W^2} (\mathcal{O}_{32}^R v_2 + 4\mathcal{O}_{33}^R v_3) g_{\mu\nu}$
34	$\Delta^{++} \Delta^{--} Z_\mu Z_\nu$	$i \frac{2g^2}{c_W^2} (c_W^2 - s_W^2)^2 g_{\mu\nu}$
35	$H^+ H^- Z_\mu Z_\nu$	$i \frac{g^2}{2c_W^2} (s_\pm^2 (c_W^2 - s_W^2)^2 + 4s_W^4 c_\pm^2) g_{\mu\nu}$
36	$G^+ G^- Z_\mu Z_\nu$	$i \frac{g^2}{2c_W^2} (c_\pm^2 (c_W^2 - s_W^2)^2 + 4s_W^4 s_\pm^2) g_{\mu\nu}$
37	$H_1 H_1 Z_\mu Z_\nu$	$i \frac{g^2}{2c_W^2} (\mathcal{O}_{12}^{R2} + 4\mathcal{O}_{13}^{R2}) g_{\mu\nu}$
38	$H_2 H_2 Z_\mu Z_\nu$	$i \frac{g^2}{2c_W^2} (\mathcal{O}_{22}^{R2} + 4\mathcal{O}_{23}^{R2}) g_{\mu\nu}$
39	$H_3 H_3 Z_\mu Z_\nu$	$i \frac{g^2}{2c_W^2} (\mathcal{O}_{32}^{R2} + 4\mathcal{O}_{33}^{R2}) g_{\mu\nu}$
40	$J J Z_\mu Z_\nu$	$i \frac{g^2}{2c_W^2} (\mathcal{O}_{12}^{I2} + 4\mathcal{O}_{13}^{I2}) g_{\mu\nu}$
41	$G^0 G^0 Z_\mu Z_\nu$	$i \frac{g^2}{2c_W^2} (\mathcal{O}_{22}^{I2} + 4\mathcal{O}_{23}^{I2}) g_{\mu\nu}$
42	$A A Z_\mu Z_\nu$	$i \frac{g^2}{2c_W^2} (\mathcal{O}_{32}^{I2} + 4\mathcal{O}_{33}^{I2}) g_{\mu\nu}$
43	$\Delta^{++} \Delta^{--} Z_\mu$	$-\frac{i g}{c_W} (c_W^2 - s_W^2) (p_1 - p_2)_\mu$
44	$H^- H^+ Z_\mu$	$\frac{i g}{2c_W} (s_\pm^2 (c_W^2 - s_W^2) - 2s_W^2 c_\pm^2) (p_1 - p_2)_\mu$
45	$G^- G^+ Z_\mu$	$\frac{i g}{2c_W} (c_\pm^2 (c_W^2 - s_W^2) - 2s_W^2 s_\pm^2) (p_1 - p_2)_\mu$
46	$H_1 J Z_\mu$	$-\frac{g}{2c_W} (\mathcal{O}_{12}^R \mathcal{O}_{12}^I - 2\mathcal{O}_{13}^R \mathcal{O}_{13}^I) (p_1 - p_2)_\mu$
47	$G^0 H_1 Z_\mu$	$\frac{g}{2c_W} (\mathcal{O}_{12}^R \mathcal{O}_{22}^I - 2\mathcal{O}_{13}^R \mathcal{O}_{23}^I) (p_1 - p_2)_\mu$
48	$A H_1 Z_\mu$	$\frac{g}{2c_W} (\mathcal{O}_{12}^R \mathcal{O}_{32}^I - 2\mathcal{O}_{13}^R \mathcal{O}_{33}^I) (p_1 - p_2)_\mu$
49	$H_2 J Z_\mu$	$-\frac{g}{2c_W} (\mathcal{O}_{22}^R \mathcal{O}_{12}^I - 2\mathcal{O}_{23}^R \mathcal{O}_{13}^I) (p_1 - p_2)_\mu$
50	$G^0 H_2 Z_\mu$	$\frac{g}{2c_W} (\mathcal{O}_{22}^R \mathcal{O}_{22}^I - 2\mathcal{O}_{23}^R \mathcal{O}_{23}^I) (p_1 - p_2)_\mu$
51	$A H_2 Z_\mu$	$\frac{g}{2c_W} (\mathcal{O}_{22}^R \mathcal{O}_{32}^I - 2\mathcal{O}_{23}^R \mathcal{O}_{33}^I) (p_1 - p_2)_\mu$
52	$H_3 J Z_\mu$	$-\frac{g}{2c_W} (\mathcal{O}_{32}^R \mathcal{O}_{12}^I - 2\mathcal{O}_{33}^R \mathcal{O}_{13}^I) (p_1 - p_2)_\mu$
53	$G^0 H_3 Z_\mu$	$\frac{g}{2c_W} (\mathcal{O}_{32}^R \mathcal{O}_{22}^I - 2\mathcal{O}_{33}^R \mathcal{O}_{23}^I) (p_1 - p_2)_\mu$
54	$A H_3 Z_\mu$	$\frac{g}{2c_W} (\mathcal{O}_{32}^R \mathcal{O}_{32}^I - 2\mathcal{O}_{33}^R \mathcal{O}_{33}^I) (p_1 - p_2)_\mu$
55	$G^\mp H^\pm Z_\mu$	$\mp \frac{g}{2c_W} c_\pm s_\pm (p_1 - p_2)_\mu$
56	$\Delta^{++} \Delta^{--} A_\mu A_\mu$	$8ie^2 g_{\mu\nu}$
57	$H^- H^+ A_\mu A_\mu$	$i 2e^2 g_{\mu\nu}$
58	$G^- G^+ A_\mu A_\mu$	$i 2e^2 g_{\mu\nu}$
59	$\Delta^{++} \Delta^{--} A_\mu$	$-2ie (p_1 - p_2)_\mu$
60	$H^+ H^- A_\mu$	$ie (p_1 - p_2)_\mu$
61	$G^+ G^- A_\mu$	$ie (p_1 - p_2)_\mu$
62	$\Delta^{++} \Delta^{--} A_\mu Z_\nu$	$4i \frac{e g}{c_W} (c_W^2 - s_W^2) g_{\mu\nu}$
63	$H^+ H^- A_\mu Z_\nu$	$i \frac{e g}{c_W} (s_\pm^2 (c_W^2 - s_W^2) - 2c_\pm^2 s_W^2) g_{\mu\nu}$
64	$G^+ G^- A_\mu Z_\nu$	$i \frac{e g}{c_W} (c_\pm^2 (c_W^2 - s_W^2) - 2s_\pm^2 s_W^2) g_{\mu\nu}$

Table III: Feynman rules for the couplings of the Higgs bosons  $H_i$  to the gauge bosons.

- 
- [1] G. Aad et al. (ATLAS Collaboration), *Observation of a new particle in the search for the Standard Model Higgs boson with the ATLAS detector at the LHC*, **Phys.Lett. B716** (2012) 1–29, arXiv:1207.7214 [hep-ex].
- [2] G. Aad et al. (ATLAS Collaboration), *Measurements of Higgs boson production and couplings in the four-lepton channel in pp collisions at center-of-mass energies of 7 and 8 TeV with the ATLAS detector* (2014), arXiv:1408.5191 [hep-ex].
- [3] V. Khachatryan et al. (CMS), *Precise determination of the mass of the Higgs boson and tests of compatibility of its couplings with the standard model predictions using proton collisions at 7 and 8 TeV*, **Eur. Phys. J. C75** (2015) 5 212, arXiv:1412.8662 [hep-ex].
- [4] G. Aad et al. (ATLAS), *Measurements of the Higgs boson production and decay rates and coupling strengths using pp collision data at  $\sqrt{s} = 7$  and 8 TeV in the ATLAS experiment* (2015), arXiv:1507.04548 [hep-ex].
- [5] M. Baak et al., *The Electroweak Fit of the Standard Model after the Discovery of a New Boson at the LHC*, **Eur. Phys. J. C72** (2012) 2205, arXiv:1209.2716 [hep-ph].
- [6] M. Baak et al. (Gfitter Group), *The global electroweak fit at NNLO and prospects for the LHC and ILC*, **Eur. Phys. J. C74** (2014) 3046, arXiv:1407.3792 [hep-ph].
- [7] M. E. Peskin and T. Takeuchi, *New constraint on a strongly interacting higgs sector*, **Phys. Rev. Lett. 65** (1990) 964–967, URL <http://link.aps.org/doi/10.1103/PhysRevLett.65.964>.
- [8] G. Altarelli and R. Barbieri, *Vacuum polarization effects of new physics on electroweak processes*, **Physics Letters B 253** (1991) 1 161 – 167, ISSN 0370-2693, URL <http://www.sciencedirect.com/science/article/pii/0370269391913789>.
- [9] M. E. Peskin and T. Takeuchi, *Estimation of oblique electroweak corrections*, **Phys. Rev. D 46** (1992) 381–409, URL <http://link.aps.org/doi/10.1103/PhysRevD.46.381>.
- [10] A. Djouadi, *The Anatomy of electro-weak symmetry breaking. I: The Higgs boson in the standard model*, **Phys.Rept. 457** (2008) 1–216, arXiv:hep-ph/0503172 [hep-ph].
- [11] C. Bonilla, R. M. Fonseca and J. W. F. Valle, *Vacuum stability with spontaneous violation of lepton number* (2015), arXiv:1506.04031 [hep-ph].
- [12] C. Bonilla, R. M. Fonseca and J. W. F. Valle, *Consistency of the triplet seesaw model revisited*, **Phys. Rev. D92** (2015) 7 075028, arXiv:1508.02323 [hep-ph].
- [13] C. Bonilla, J. W. F. Valle and J. C. Romão, *Neutrino mass and invisible Higgs decays at the LHC*, **Phys. Rev. D91** (2015) 11 113015, arXiv:1502.01649 [hep-ph].
- [14] J. Schechter and J. Valle, *Neutrino Decay and Spontaneous Violation of Lepton Number*, **Phys.Rev. D25** (1982) 774.
- [15] A. S. Joshipura and J. Valle, *Invisible Higgs decays and neutrino physics*, **Nucl.Phys. B397** (1993) 105–122.
- [16] M. A. Diaz, M. Garcia-Jareno, D. A. Restrepo and J. Valle, *Seesaw Majoron model of neutrino*

- mass and novel signals in Higgs boson production at LEP*, *Nucl.Phys.* **B527** (1998) 44–60, arXiv:hep-ph/9803362 [hep-ph].
- [17] Y. Chikashige, R. N. Mohapatra and R. Peccei, *Are There Real Goldstone Bosons Associated with Broken Lepton Number?*, *Phys.Lett.* **B98** (1981) 265.
  - [18] G. Gelmini and M. Roncadelli, *Left-Handed Neutrino Mass Scale and Spontaneously Broken Lepton Number*, *Phys.Lett.* **B99** (1981) 411.
  - [19] R. E. Shrock and M. Suzuki, *Invisible Decays of Higgs Bosons*, *Phys. Lett.* **B110** (1982) 250.
  - [20] S. M. Boucenna, S. Morisi and J. W. Valle, *The low-scale approach to neutrino masses*, *Adv.High Energy Phys.* **2014** (2014) 831598, arXiv:1404.3751 [hep-ph].
  - [21] J. Schechter and J. Valle, *Neutrino Masses in  $SU(2) \times U(1)$  Theories*, *Phys.Rev.* **D22** (1980) 2227.
  - [22] K. Kannike, *Vacuum Stability Conditions From Copositivity Criteria*, *Eur.Phys.J.* **C72** (2012) 2093, arXiv:1205.3781 [hep-ph].
  - [23] K. A. Olive et al. (Particle Data Group), *Review of Particle Physics*, *Chin. Phys.* **C38** (2014) 090001.
  - [24] K. Choi and A. Santamaria, *Majorons and Supernova Cooling*, *Phys.Rev.* **D42** (1990) 293–306.
  - [25] V. Khachatryan et al. (CMS Collaboration), *Observation of the diphoton decay of the Higgs boson and measurement of its properties*, *Eur.Phys.J.* **C74** (2014) 10 3076, arXiv:1407.0558 [hep-ex].
  - [26] G. Aad et al. (ATLAS, CMS), *Combined Measurement of the Higgs Boson Mass in  $pp$  Collisions at  $\sqrt{s} = 7$  and 8 TeV with the ATLAS and CMS Experiments*, *Phys. Rev. Lett.* **114** (2015) 191803, arXiv:1503.07589 [hep-ex].
  - [27] J. Abdallah et al. (DELPHI Collaboration), *Searches for neutral higgs bosons in extended models*, *Eur.Phys.J.* **C38** (2004) 1–28, arXiv:hep-ex/0410017 [hep-ex].
  - [28] *Measurements of the Higgs boson production and decay rates and constraints on its couplings from a combined ATLAS and CMS analysis of the LHC  $pp$  collision data at  $\sqrt{s} = 7$  and 8 TeV*, Technical Report ATLAS-CONF-2015-044, CERN, Geneva (2015), URL <http://cds.cern.ch/record/2052552>.
  - [29] V. Khachatryan et al. (CMS), *Search for a Higgs Boson in the Mass Range from 145 to 1000 GeV Decaying to a Pair of  $W$  or  $Z$  Bosons* (2015), arXiv:1504.00936 [hep-ex].
  - [30] V. Khachatryan et al. (CMS), *Search for neutral MSSM Higgs bosons decaying to a pair of tau leptons in  $pp$  collisions*, *JHEP* **10** (2014) 160, arXiv:1408.3316 [hep-ex].
  - [31] G. Aad et al. (ATLAS), *Search for Scalar Diphoton Resonances in the Mass Range 65 – 600 GeV with the ATLAS Detector in  $pp$  Collision Data at  $\sqrt{s} = 8$  TeV*, *Phys. Rev. Lett.* **113** (2014) 17 171801, arXiv:1407.6583 [hep-ex].
  - [32] V. Khachatryan et al. (CMS), *Search for diphoton resonances in the mass range from 150 to 850 GeV in  $pp$  collisions at  $\sqrt{s} = 8$  TeV*, *Phys. Lett.* **B750** (2015) 494–519, arXiv:1506.02301 [hep-ex].

- [33] G. Aad et al. (ATLAS), *Search for a CP-odd Higgs boson decaying to  $Zh$  in  $pp$  collisions at  $\sqrt{s} = 8$  TeV with the ATLAS detector*, *Phys. Lett.* **B744** (2015) 163–183, arXiv:1502.04478 [hep-ex].
- [34] J. Garayoa and T. Schwetz, *Neutrino mass hierarchy and Majorana CP phases within the Higgs triplet model at the LHC*, *JHEP* **03** (2008) 009, arXiv:0712.1453 [hep-ph].
- [35] P. Fileviez Perez et al., *Testing a Neutrino Mass Generation Mechanism at the LHC*, *Phys.Rev.* **D78** (2008) 071301, arXiv:0803.3450 [hep-ph].
- [36] P. Fileviez Perez et al., *Neutrino Masses and the CERN LHC: Testing Type II Seesaw*, *Phys.Rev.* **D78** (2008) 015018, arXiv:0805.3536 [hep-ph].
- [37] F. del Aguila and J. A. Aguilar-Saavedra, *Distinguishing seesaw models at LHC with multi-lepton signals*, *Nucl. Phys.* **B813** (2009) 22–90, arXiv:0808.2468 [hep-ph].
- [38] M. Aoki, S. Kanemura and K. Yagyu, *Testing the Higgs triplet model with the mass difference at the LHC*, *Phys. Rev.* **D85** (2012) 055007, arXiv:1110.4625 [hep-ph].
- [39] A. G. Akeroyd and S. Moretti, *Enhancement of  $H$  to  $\gamma\gamma$  from doubly charged scalars in the Higgs Triplet Model*, *Phys. Rev.* **D86** (2012) 035015, arXiv:1206.0535 [hep-ph].
- [40] P. S. Bhupal Dev, D. K. Ghosh, N. Okada and I. Saha, *125 GeV Higgs Boson and the Type-II Seesaw Model*, *JHEP* **03** (2013) 150, [Erratum: JHEP05,049(2013)], arXiv:1301.3453 [hep-ph].
- [41] F. del Águila and M. Chala, *LHC bounds on Lepton Number Violation mediated by doubly and singly-charged scalars*, *JHEP* **03** (2014) 027, arXiv:1311.1510 [hep-ph].
- [42] C.-H. Chen and T. Nomura, *Search for  $\delta^{\pm\pm}$  with new decay patterns at the LHC*, *Phys. Rev.* **D91** (2015) 035023, arXiv:1411.6412 [hep-ph].
- [43] S. Kanemura, M. Kikuchi, K. Yagyu and H. Yokoya, *Bounds on the mass of doubly-charged Higgs bosons in the same-sign diboson decay scenario*, *Phys. Rev.* **D90** (2014) 11 115018, arXiv:1407.6547 [hep-ph].
- [44] Z.-L. Han, R. Ding and Y. Liao, *LHC Phenomenology of Type II Seesaw: Nondegenerate Case*, *Phys. Rev.* **D91** (2015) 093006, arXiv:1502.05242 [hep-ph].
- [45] H. Sugiyama, K. Tsumura and H. Yokoya, *Discrimination of models including doubly charged scalar bosons by using tau lepton decay distributions*, *Phys. Lett.* **B717** (2014) 229–234, arXiv:1207.0179 [hep-ph].
- [46] S. Chatrchyan et al. (CMS), *A search for a doubly-charged Higgs boson in  $pp$  collisions at  $\sqrt{s} = 7$  TeV*, *Eur. Phys. J.* **C72** (2012) 2189, arXiv:1207.2666 [hep-ex].
- [47] G. Aad et al. (ATLAS), *Search for doubly-charged Higgs bosons in like-sign dilepton final states at  $\sqrt{s} = 7$  TeV with the ATLAS detector*, *Eur. Phys. J.* **C72** (2012) 2244, arXiv:1210.5070 [hep-ex].
- [48] S. Kanemura, K. Yagyu and H. Yokoya, *First constraint on the mass of doubly-charged Higgs bosons in the same-sign diboson decay scenario at the LHC*, *Phys. Lett.* **B726** (2013) 316–319, arXiv:1305.2383 [hep-ph].

- [49] S. Kanemura, M. Kikuchi, H. Yokoya and K. Yagyu, *LHC Run-I constraint on the mass of doubly charged Higgs bosons in the same-sign diboson decay scenario*, **PTEP** **2015** (2015) **051B02**, arXiv:1412.7603 [hep-ph].
- [50] V. Khachatryan et al. (CMS), *Study of vector boson scattering and search for new physics in events with two same-sign leptons and two jets*, **Phys. Rev. Lett.** **114** (2015) 5 051801, arXiv:1410.6315 [hep-ex].
- [51] D. Fontes, J. C. Romão and J. P. Silva,  *$h \rightarrow Z\gamma$  in the complex two Higgs doublet model*, **JHEP** **12** (2014) **043**, arXiv:1408.2534 [hep-ph].
- [52] G. Aad et al. (ATLAS), *Search for invisible decays of a Higgs boson using vector-boson fusion in pp collisions at  $\sqrt{s} = 8$  TeV with the ATLAS detector* (2015), arXiv:1508.07869 [hep-ex].
- [53] S. Chatrchyan et al. (CMS), *Search for invisible decays of Higgs bosons in the vector boson fusion and associated ZH production modes*, **Eur. Phys. J.** **C74** (2014) 2980, arXiv:1404.1344 [hep-ex].
- [54] G. Passarino and M. J. G. Veltman, *One loop corrections for  $e^+e^-$  annihilation into  $\mu^+\mu^-$  in the Weinberg model*, **Nucl. Phys.** **B160** (1979) 151–207, URL <http://www.sciencedirect.com/science/article/pii/0550321379902347>.